Large-Signal Network Analysis

"Going beyond S-parameters"

Dr. Jan Verspecht

"Jan Verspecht bvba"
URL: http://www.janverspecht.com

This presentation contains several slides which are used with the permission of Agilent Technologies, Inc.

Outline

- Part I
  - Introduction
  - Instrumentation and Calibration
- Break
  - Coffee and Cookies
- Part II
  - Applications
  - Conclusions

Let us start by giving the outline of this presentation.

The presentation has two parts.

In the first part we will give an introduction to the subject of “Large-Signal Network Analysis”.

We will discuss the hardware and calibration aspects of the “Large-Signal Network Analyzer” measurement instrument.

After the break, we will start the second part of the talk.

We will present several different applications of “Large-Signal Network Analysis”. The applications presented are time domain waveform measurements of voltage and current, physical model improvement and black-box modeling techniques, in the time as well as in the frequency domain.

The presentation ends with a short conclusion.

Part I - Outline

- Introduction
- Signal Representations
- Instrumentation Hardware
- Calibration Aspects

A more detailed outline of Part I is given in what follows.

We will introduce the subject by defining what we mean by the expression “Large-Signal Network Analysis”.

Next we will present the different ways of representing signals. Where as a single frequency domain S-parameter formalism is sufficient for the classical “small-signal network analysis”, we will show that more mathematical tools are needed to describe and interpret the data resulting from “large-signal network analysis”.

We will then discuss the “Large-Signal Network Analyzer” (LSNA) instrumentation hardware: what components and architecture is used and what are the basic principles of operation?

Next we will show how to extend the classical network analyzer calibration in order to deal with the accurate measurement of large-signal behavior and how these calibration aspects relate to the work which is presently being done at the NIST in Boulder (Colorado - USA).

Large-Signal Network Analysis?

- Put a D.U.T. (“network”) in realistic large-signal operating conditions
- Completely and accurately characterize the D.U.T. behavior
- Analyze the D.U.T. behavior using the measured data

The S-parameter theory and the associated instrumentation revolutionized the high-frequency electronic industry. In fact S-parameters got so ingrained that many people believe they are omnipotent when it comes to solving microwave problems. One can not repeat enough, however, that their applicability is strictly limited to cases where the superposition theorem holds. In other words, S-parameters are only useful to describe linear behavior.

For semi-conductor components this implies that the signal levels need to be small. Many applications today require the usage of signal levels which are significantly higher, e.g. power amplifiers. There is as such a need to “go beyond S-parameters”. We call the realized ensemble of measuring and modeling solutions “Large-Signal Network Analysis”.

In Part I we will mainly focus on the measurement solutions. The idea is to put a device-under-test (DUT) under realistic large-signal operating conditions and to acquire complete and accurate information of its electrical behavior.

Having the right tools, it is then possible to analyze the network behavior. This is discussed in Part II.

Part I - Outline

- Introduction
- Signal Representations
- Instrumentation Hardware
- Calibration Aspects

We will present the different ways of representing signals. Where as a single frequency domain S-parameter formalism is sufficient for the classical “small-signal network analysis”, we will show that more mathematical tools are needed to describe and interpret the data resulting from “large-signal network analysis”.

Signal Representations

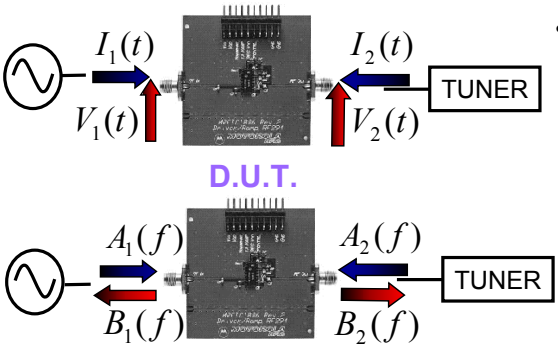

- Set of Physical Quantities
  - Traveling Waves (A, B)
  - Voltage/Current (V, I)
- Representation Domain
  - Frequency (f)
  - Time (t)
  - Envelope (f,t)

- LSNA is capable of periodic and periodically modulated signals

The realistic operating conditions are typically achieved by stimulating the device with synthesizers and by using active and/or passive tuning techniques.

Unlike S-parameters, different choices can be (need to be) made for the representation of the acquired data. The best choice will depend on the application.

On the next slide we discuss the use of a “traveling voltage waves” or a “voltage/current” representation.

On the following slides we will talk about the signal classes that can be measured by the present LSNA instrumentation: periodic signals and periodically modulated signals.

We will also show how different “domains” can be used to represent the same data: the time domain, the frequency domain and the envelope domain.

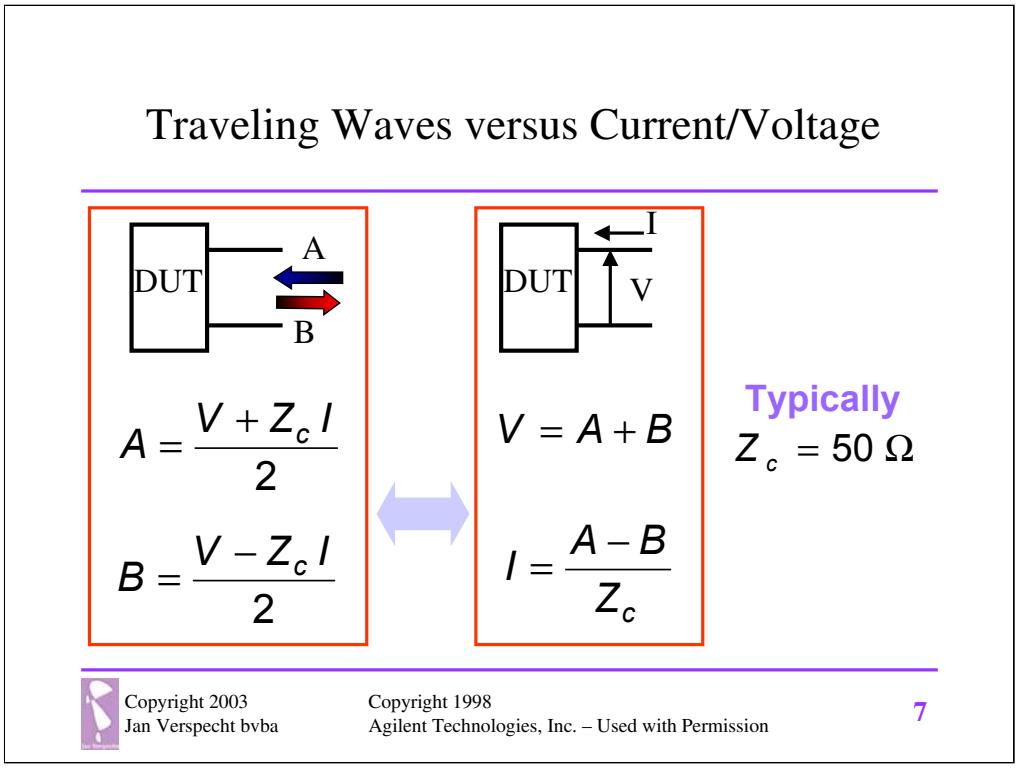

As we said before, the LSNA will return the measured data as a port current (noted I) and a port voltage (noted V), or as an incident (noted A) and a scattered (noted B) traveling voltage wave at that port. Since we assume that we are dealing with a quasi-TEM mode of propagation the relationship between both sets of quantities is given by the simple linear transformation represented above.

A-B representations are typically used for near matched and distributed applications (system amplifier).

V-I representations are typically used for lumped non-matched applications (individual transistors).

In most cases a characteristic impedance of 50 Ohms is used for the wave definition. For certain applications, however, other values can be more useful. In general, Z_c can be frequency dependent. An example is the black-box modeling of the behavior of a power transistor. In this case it is convenient to represent the fundamental at the output in an impedance which is close to the optimal match (typically a few Ohms).

Several other different conventions to define traveling waves are defined in technical literature. An excellent reference paper on this issue: R. B. Marks and D. F. Williams, "A general waveguide circuit theory," Journal of Research of the National Institute of Standards and Technology, vol. 97, pp. 533-562, Sept.-Oct. 1992. In the light of this paper the traveling voltage wave definitions we use are so-called pseudo-waves. This is the case since the characteristic impedance does not correspond to the characteristic impedance of a physical waveguide, but is used as a mathematical normalization factor. Note that the formulation that we use is compatible with commercial vector network analyzer definitions of S-parameters.

Signal Class: CW Signals

- 2-port DUT under periodic excitation
- E.g. transistor excited by a 1 GHz tone with an arbitrary output termination
- All current and voltage waveforms are represented by a fundamental and harmonics

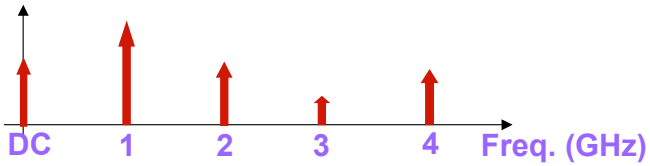

- Spectral components X_h = complex Fourier Series coefficients of the waveforms

In what follows we will explain what type of signals can be acquired with the present state-of-the-art LSNA instrumentation.

The simplest measurement capability deals with continuous wave one-tone excitation of 2-port devices, e.g. a biased FET-transistor excited by a 1GHz CW signal at the gate, with an arbitrary load at the drain.

Assuming that the device is stable (not oscillating) and does not exhibit subharmonic or chaotic behavior, all current and voltage waveforms will have the same periodicity as the drive signal, in this case 1 ns.

This implies that all voltage and current waveforms (or the associated traveling voltage waves) can be represented by their complex Fourier series coefficients. These are called the spectral components or phasors. One calls the 1GHz component the fundamental, the 2GHz component the 2nd harmonic, the 3GHz component the 3rd harmonic,… The DC components are called the DC-bias levels.

The measurement problem is as such defined as the determination of the phase and amplitude of the fundamental and the harmonics, together with the measurement of the DC-bias. The set of frequencies which is measured is called the LSNA “frequency grid”. All frequencies of the grid are uniquely determined by an integer (h), called the “harmonic index”.

In theory an infinite number of harmonics exist. In all practical cases, however, the power in each harmonic rapidly decreases when the harmonic index increases. It is as such sufficient to measure the harmonics only up to a certain harmonic index.

CW: Time and Frequency Domain

$$x(t) = \mathrm{Re}\left(\sum_{h=0}^{H} X_h \, e^{j\,2\pi h f t} \right)$$

$$X_h = 2f \int_0^{f^{-1}} x(t) e^{-j\,2\pi h f t} dt$$

$$f = 1/\,period = fundamental\ frequency$$

For the single harmonic grid the necessary time-to-frequency domain transformations are given by the above formulas, which are just one way to write the Fourier and inverse-Fourier transformation. Note that other conventions are also in use. We use Volt-peak for the amplitudes and a negative linear phase for denoting a positive delay (typical electrical engineering convention). This convention is compatible with commercial CAD tools.

It may be interesting to note that time domain representations are typically used for V-I representations to study the behavior of small “lumped” transistors, where frequency domain representations are typically used for A-B representations to study the behavior of larger “distributed” systems.

Time Domain V/I Representation

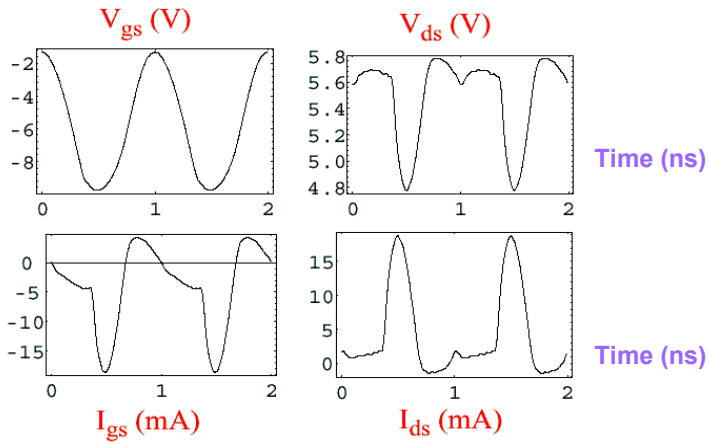

As a practical example of a time domain representation, consider the picture above.

The figures represent the voltage and current waveforms at the gate and drain of a FET transistor excited by a large 1GHz signal.

Note that the equivalent information is represented in the frequency domain by 4 lists, with each list containing 21 complex numbers (the values of the spectral components up to 20GHz, including DC).

The physical interpretation of the data will be clarified later in the presentation.

Signal Class: Modulated Signals

- Periodically modulated version of the previous case
- e.g. transistor excited by a modulated 1 GHz tone (modulation period = 10 kHz)

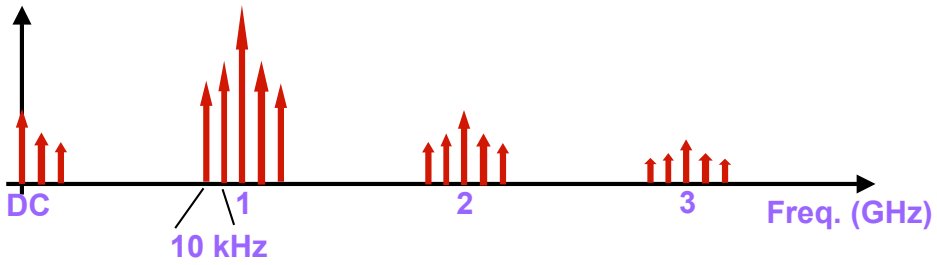

- Spectral components X

Another type of signals that can be measured with an LSNA is the periodically modulated version of the previous example of a CW signal. As an example, consider the same FET transistor whereby one modulates the 1GHz signal source, such that the modulation has a period of 10kHz.

The voltage and current waveforms will now contain many more spectral components. New components will arise at integer multiples of 10kHz offset relative to the harmonic frequency grid. In practice significant energy will only be present in a limited bandwidth around each harmonic.

The resulting set of frequencies is called a “dual frequency grid”. Note that in this case each frequency is uniquely determined by a set of two integers, one denoting the harmonic frequency, and one denoting the modulation frequency. E.g. harmonic index (3,-5) denotes the frequency 3GHz - 50kHz.

The measurement problem will be to determine the phase and the amplitude of all relevant spectral components of current and voltage.

Modulation: Time and Frequency Domain

$$x(t) = \mathrm{Re}\left(\sum_{h=0}^{H} \sum_{m=-M}^{+M} X_{hm}\, e^{j\,2\pi\,(h f_C + m f_M)\,t} \right)$$

$$X_{hm} = \lim_{T \to \infty} \frac{1}{T} \int_{-T}^{T} x(t) e^{-j\,2\pi (h f_C + m f_M) t}\, dt$$

f_C = carrier frequency

f_M = modulation frequency

The transformation between the time and the frequency domain gets more complex for the periodically modulated case. Note that one now has to take into account two frequencies: the carrier frequency and the modulation frequency.

Note that the formulation of the Fourier transform (the 2nd equation) contains a limit to infinity. This formulation is necessary since the time domain signals are in general no longer periodic but so-called pseudo-periodic. This is the case since the carrier frequency and the modulation frequency can, in general, not be written as integer multiples of a common "fundamental" frequency (they are "non-commensurate"). As such the usual Fourier series expansion formula can no longer be used, this is only possible in the case of the single frequency grid.

Modulation: Envelope Domain

$$x(t) = \mathrm{Re}\left(\sum_{h=0}^{H} X_h(t) e^{j\,2\pi h f_c t} \right)$$

$$X_h(t) = \sum_{m=-M}^{M} X_{hm}\, e^{j\,2\pi m f_M t}$$

Next to the frequency and time domain, other representations can be useful for describing modulated measurements. One commonly used example is the so-called “envelope domain”. This representation is used in so-called “envelope simulators”. The idea is to write the signal as the superposition of a set of time-dependent complex phasors. One has one time-dependent phasor for each of the RF carriers, in our case the fundamental and all of the harmonics.

These complex time domain functions are often called IQ-traces, where I refers to their real part and Q to their imaginary part. This representation is very natural to digital modulation people. An appropriately sampled IQ-trace results e.g. in one of the typical constellation diagrams, such as 16-QAM,…

The mathematical definition of these phasor representations (one complex function of time for each harmonic) is given by the above formula.

Modulation: Time and Envelope Domain

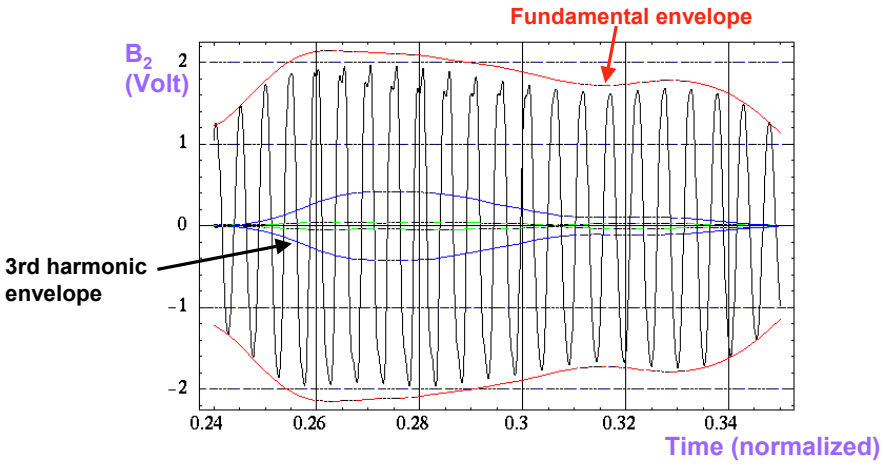

The above figure illustrates the time domain and envelope domain representations. It represents a part of the output wave of an RFIC which is excited by a modulated 1.8GHz carrier at the input. The modulation format used has statistical characteristics similar to those of a true CDMA signal.

The oscillating waveform is the time domain representation. This waveform does not correspond, however, with the physical signal. In reality hundreds of carrier oscillations occur before there is any noticeable deviation in the envelope. As such a realistic representation would look like a black blur of ink. In order to interpret the time domain data, the ratio between the modulation time constant (microseconds) and the carrier time constant (nanoseconds) is artificially decreased. This allows to visualize how the carrier waveform changes throughout the envelope. Note for instance the clipping which occurs at the highest amplitudes.

The other, smoother, traces which also occur on the figure are the amplitudes of the time dependent phasor representations of the fundamental and the 2nd and 3rd harmonic. Note how the amplitude of the fundamental phasor becomes larger than the peak-voltage of the time domain waveform at the high amplitudes. This is the well known typical behavior for a clipped waveform. It can be explained by the presence of a significant third harmonic, which is in opposite phase relative to the fundamental. Note that the measured time-dependent phase characteristics are not indicated on the figure for reasons of clarity.

Modulation: Frequency Domain

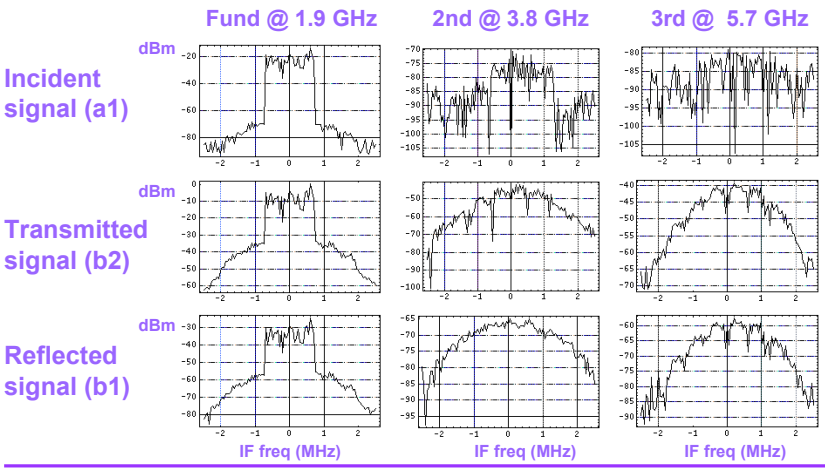

This figure represents a full frequency domain representation of the measured data for the same DUT and experimental conditions as on the previous slide.

We see the amplitude of all modulation components around the fundamental, the 2nd and the 3rd harmonic, and this for the incident wave a_1, as well as for the transmitted wave b_2 and the reflected wave b_1. This representation is useful for studying typical nonlinear frequency domain effects like e.g. spectral regrowth.

Modulation: 2D Time Domain

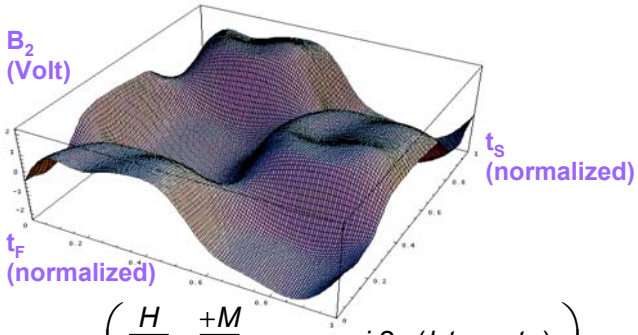

$$x_{2D}(t_F, t_S) = \mathrm{Re}\left(\sum_{h=0}^{H} \sum_{m=-M}^{+M} X_{hm}\, e^{j\,2\pi(h t_F + m t_S)} \right)$$

$$x(t) = x_{2D}(f_c t, f_M t)$$

An original way of representing the modulated data is illustrated above. The signal is represented by means of a 2-dimensional time domain function. There is one time axis for the RF carrier fundamental and harmonics (RF time or fast time, denoted t_F) and another time axis for the envelope (envelope time or slow time, denoted t_S). This kind of data representation is used by advanced research simulators.

Making a cut perpendicular to the t_S axis (t_S = constant) shows how the RF waveform looks like at that particular instance of the envelope time. Scanning through the whole range of t_S shows how the RF waveform changes throughout the envelope.

The example shown above represents the output of an amplifier driven by a 2-tone signal. One can clearly see how the waveform clips at the higher amplitudes.

Looking at the mathematical formulation one notes that this 2-dimensional waveform is actually the inverse discrete 2-dimensional Fourier transform of the spectral components (where one treats the modulation index as a second dimension).

As shown on the slide the physical time signal is retrieved by evaluating the 2D function in the de-normalized fast time and slow time variables.

Part I - Outline

- Introduction
- Signal Representations
- Instrumentation Hardware
- Calibration Aspects

We continue with demystifying the hardware components and high-level architecture of an LSNA instrument.

Hardware: Historical Overview

- 1988 Markku Sipila & al.: 2 channel scope with one coupler at the input (14 GHz)
- 1989 Kompa & Van Raay: 2 channel scope with VNA test-set + receiver
  Lott: VNA test set + receiver (26.5 GHz)
- 1992 Kompa & Van Raay: test-set with MTA (40 GHz)
  Verspecht & al.: 4 couplers with a 4 channel oscilloscope (20 GHz)
- 1994 Demmler, Tasker, Leckey, Wei, Tkachenko:
  test-set with MTA (40 GHz)
  Verspecht & al.: 4 couplers with 2 synchronized MTA's
- 1996 Verspecht & al.: NNMS, 4 couplers, 4 channel converter, 4 ADC's
- 1998 Nebus & al.: VNA test set + receiver with loadpull and pulsed capability
- 2003 Maury Microwave, Inc.: commercial introduction (LSNA)

First an historical overview of the evolution of the hardware is given. In 1988 Markku Sipila reports of a measurement system to measure the voltage and current waveforms at the gate and drain of a HF transistor. He uses a 2-channel 14GHz oscilloscope and one coupler at the input.

In 1989 Kompa & Van Raay report on a similar set-up based upon a 2-channel scope combined with a complete VNA test-set and receiver. The receiver is used to measure the fundamental data, the scope is used for the harmonics. The same year Urs Lott reports on a system which is based exclusively on a VNA test-set and receiver. He measures the harmonics with the receiver by tuning it consecutively to each of the harmonics. An ingenious phase reference method is used to align the harmonic phases (the so-called "golden diode" approach) .

A breakthrough takes place in 1992 with the introduction of the Hewlett-Packard "Microwave Transition Analyzer". This is a 40GHz 2-channel receiver which allows the direct measurement of fundamental and harmonic phasors. It is first used by Kompa & Van Raay. In 1994 it is also used by Demmler, Tasker, Leckey, Wei and Tkachenko. Hewlett-Packard's "Network Measurement and Dewcription Group" uses 2 MTA's as a 4-channel harmonic receiver.

In 1996 NMDG leverages hardware from the MTA instrument and builds the "Nonlinear-Network Measurement System", later to be called the "Large-Signal Network Analyzer".

In 1998 Nebus builds a VNA receiver system with loadpull and pulsed measurement capability (using a phase reference similar to Urs Lott).

In 2000 Verspecht adds modulation capability to the LSNA.

In 2003 Maury Microwave, Inc. starts commercializing LSNA instruments.

Architecture of the LSNA prototype

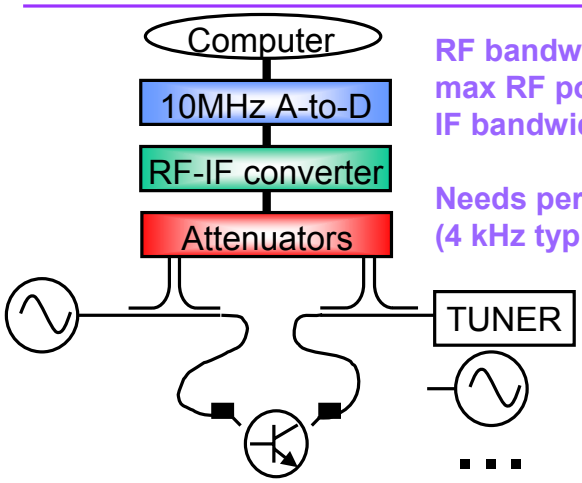

RF bandwidth: 600MHz - 50GHz
max RF power: 10 Watt
IF bandwidth: 8 MHz

Needs periodic modulation
(4 kHz typical)

The hardware architecture of the LSNA is relatively simple.

4 couplers are used for sensing the spectral components of the incident and scattered voltage waves at both DUT ports. The sensed signals are attenuated to an acceptable level before being sent to the input channels of a 4 channel broadband frequency converter. This RF-IF converter is based upon the harmonic sampling principle and converts all of the spectral components coherently to a lower frequency copy (below 4MHz). The input bandwidth is 50GHz.

The resulting IF signals are digitized by a set of 4 high-performance analog-to-digital converters (ADCs). A computer does all the processing which is needed to finally end up with the calibrated data in the preferred format (A/B or V/I, time, frequency or envelope domain).

The specifications of the LSNA at present: the calibrated RF frequency range equals 600MHz-50GHz, the maximum RF power equals 10Watt, the maximum bandwidth of the modulated signal equals 8MHz. The repetition frequency of the modulation is typically a few kHz.

Note that synthesizers and tuners for the signal generation can be (need to be) added externally. They are not considered as being part of the LSNA.

Although not shown above for reasons of simplicity, DC bias circuitry is also present in the LSNA.

RF-IF converter: Simplified Schematic

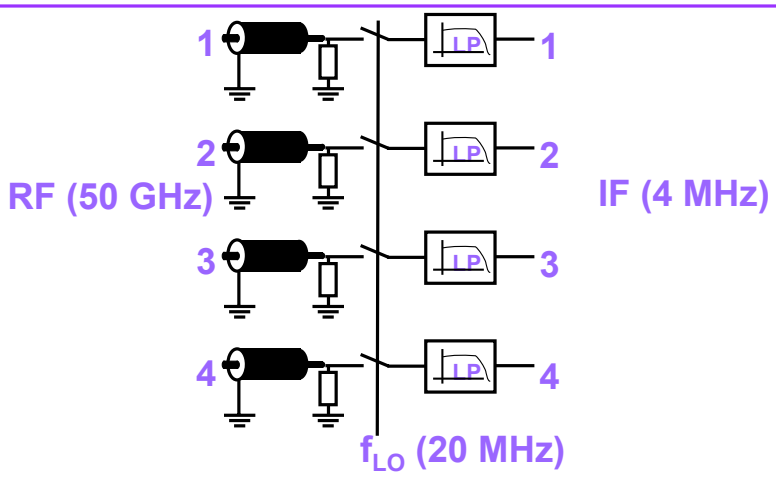

The 4-channel RF-IF sampling frequency converter is the core of the LSNA. It is based on broadband sampler technology.

One digital synthesizer drives 4 sampler switches at a rate close to 20MHz. This rate will be called the local oscillator frequency or f_{LO} in what follows. Each time the switch closes for a duration of about 10 ps it samples a little bit of charge and sends it to a low pass filter. When the synthesizer frequency is properly chosen, one finds a low frequency copy of all input spectral components at the output of the filter.

In order to understand the principle of harmonic sampling it is important to know that the sampling process of a signal is expressed in the frequency domain as a convolution with a Dirac-delta comb, with a spacing equal to f_{LO}.

Harmonic Sampling - Signal Class: CW

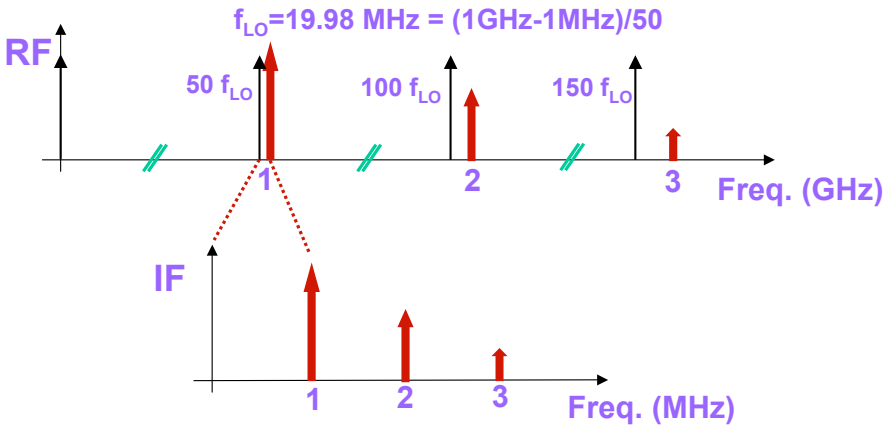

The harmonic sampling idea is best illustrated for the case of a single frequency grid.

Assume that we need to measure a 1GHz fundamental together with its 2nd and 3rd harmonic. We choose a local oscillator (LO) frequency of 19.98MHz. The 50th harmonic of the LO will equal 999MHz. This component mixes with the fundamental and results in a 1MHz mixing product at the output of the converter. The 100th harmonic of the LO equals 1998MHz, it mixes with the 2nd harmonic at 2GHz and results in a 2MHz mixing product. The 150th harmonic of the LO equals 2997MHz, it mixes with the third harmonic at 3GHz and results in a 3MHz mixing product.

The final result at the output of the converter is a 1MHz fundamental together with its 2nd and 3rd harmonic. This is actually a low frequency copy of the high frequency RF signal. This signal is then digitized, and the values of the spectral components are extracted by applying a discrete Fourier transformation.

The process for a modulated signal is very similar but more complex. After the RF-IF conversion all harmonics and modulation tones can be found back in the IF channel, ready for digitizing and processing.

Part I - Outline

- Introduction
- Signal Representations
- Instrumentation Hardware
- Calibration Aspects

As the last item in Part I we will discuss the calibration aspects of an LSNA.

Calibration: Historical Overview

- 1988 VNA-like characterization of the test-set
  power calibration with a power meter
  assumption of an ideal-phase receiver
- 1989 phase calibration by the "golden diode" approach (Urs Lott)
- 1994 harmonic phase calibration with a characterized SRD, traceable to a nose-to-nose calibrated sampling oscilloscope (Verspecht)
- 2000 IF calibration (Verspecht)
- 2000 NIST investigates "phase reference generator" approach (DeGroot)
- 2001 calibrated electro-optical sampling (D.F. Williams, P. Hale @ NIST)
  (provides better harmonic phase accuracy than nose-to-nose)

Inevitably all of the RF hardware components introduce significant distortions. These have to be compensated by calibration procedures.

A short historical overview follows.

In 1988, Markku Sipila (2-channel scope with one coupler) used a VNA-like characterization of the test-set, and an amplitude calibration with a power meter. He assumes that the oscilloscope has an ideal linear phase characteristic.

In 1989 Urs Lott (VNA test-set and receiver for fundamental and harmonics) uses a "golden diode" approach in order to align the phases of the harmonics and the fundamental.

In 1994 Hewlett-Packard NMDG calibrates the phase distortion of their set-up by means of a "phase reference generator". This is a step-recovery-diode pulse generator which is characterized by a sampling oscilloscope, which itself is calibrated using the "nose-to-nose" technique.

In 2000 an IF-calibration is added to the LSNA. This is necessary for performing accurate measurements under modulated signal conditions. During the same year Don DeGroot of NIST starts investigating the "harmonic phase reference generator" approach.

In 2001 D. F. Williams and P. Hale succeed in calibrating a broadband (110 GHz) electro-optic sampling system. This system can be used as a more accurate harmonic phase standard than the nose-to-nose calibration procedure.

Raw Quantities versus DUT Quantities

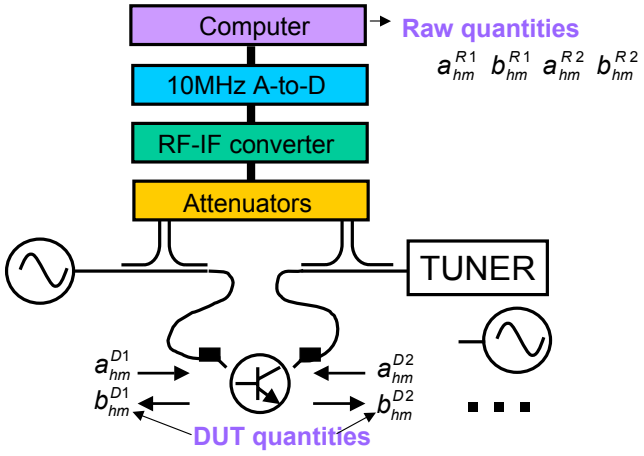

Before continuing with the calibration aspects it is useful to revisit the hardware schematic of an LSNA.

During an experiment we want to know the phases and amplitudes of a discrete set of spectral components at the DUT signal ports.

These quantities are called the ”DUT quantities” and are denoted by a superscript “D”.

Unfortunately we do not have direct access to these quantities. The only information we can get are the uncalibrated measured values. These are called the “raw quantities” and are denoted by a superscript “R”.

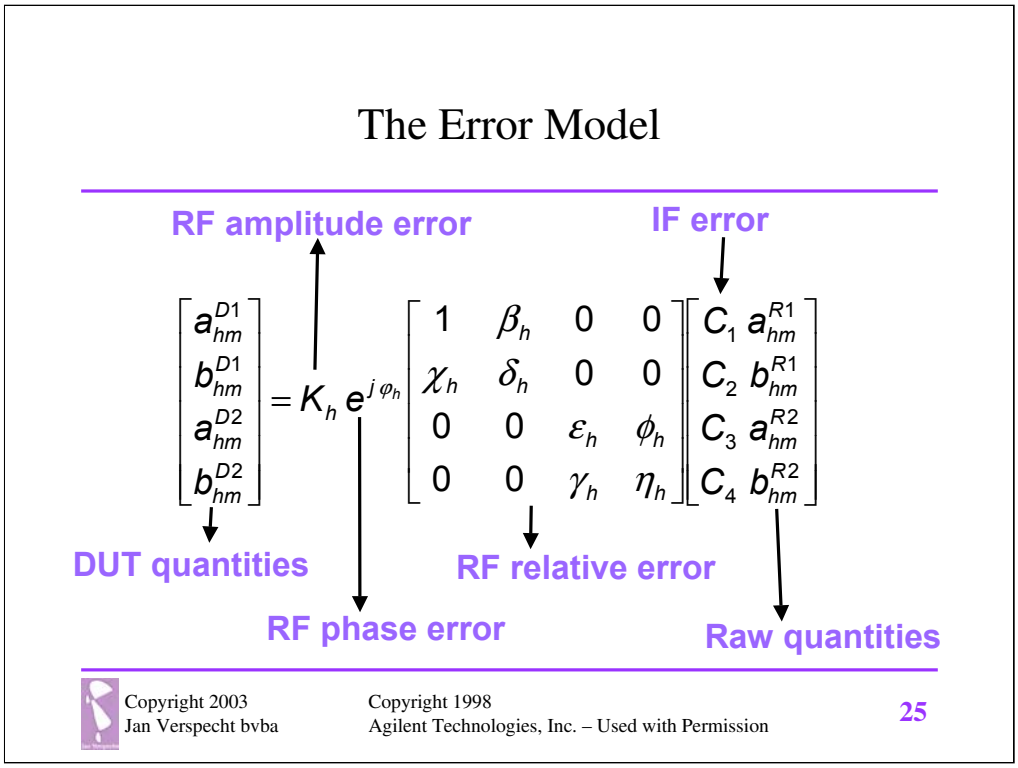

Each calibration starts with an error model. The mathematical description we use is given above.

The main assumption is that there exists a linear relationship between the raw measured spectral components and the actual spectral components at the DUT signal ports. The relationship can be described by the above formulation.

It is assumed that the error has two independent sources of error: a high frequency (RF) error, caused by all of the RF hardware up to the sampling switch, and a low frequency (IF) error which is caused by the low pass filter characteristic of the RF-IF converter and the transfer characteristic of the analog-to-digital converters.

First the IF correction is applied to the raw data. This correction is indicated by the variables C_1, C_2, C_3 and C_4.

Next the RF correction is applied. It is described by a 16-element matrix. Note that 8 zero's are present. This corresponds to the assumption that there is no cross-coupling between port 1 and port 2.

The elements of the matrix are determined in three steps: a classical VNA calibration (to determine the "RF relative error"), an amplitude calibration and an harmonic phase calibration. Note that one needs to determine this matrix for each of the harmonics to be measured.

RF Calibration

1. Coaxial SOLT calibration

   OR

   On wafer LRRM calibration

Combined with

2. HF amplitude calibration with power meter
3. HF harmonic phase calibration with a SRD diode (characterized by a nose-to-nose calibrated sampling oscilloscope)

The RF error is related to the high frequency hardware (couplers, cables, probes) and is much more sensitive to external influences than the IF error. It is recommended to perform this calibration before each measurement session and at least once a day.

For coaxial measurements a classical SOLT procedure is used for determining the relative error, while an LRRM is being used for on wafer measurements.

The amplitude calibration is performed by means of a power meter and the harmonic phase calibration by means of a phase reference generator. A phase reference generator is a step-recovery-diode pulse generator which has been characterized by a sampling oscilloscope, which on his turn has been calibrated by a nose-to-nose calibration procedure (explained in what follows).

Coaxial Amplitude and Phase Calibration

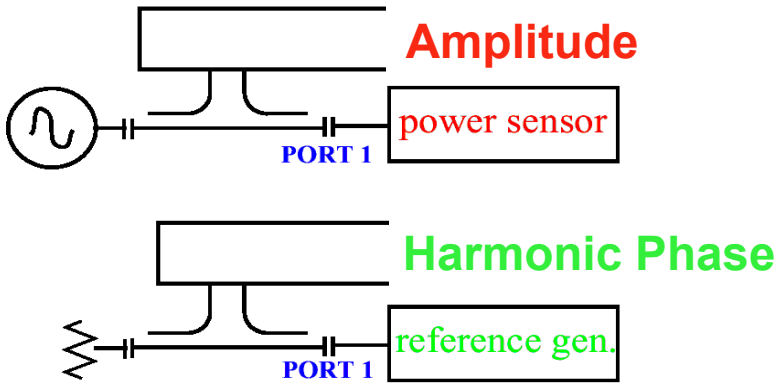

During a coaxial calibration one connects the power sensor and the reference generator directly to one of the analyzer signal ports. They can be considered as additional calibration elements.

On Wafer Amplitude & Phase Calibration

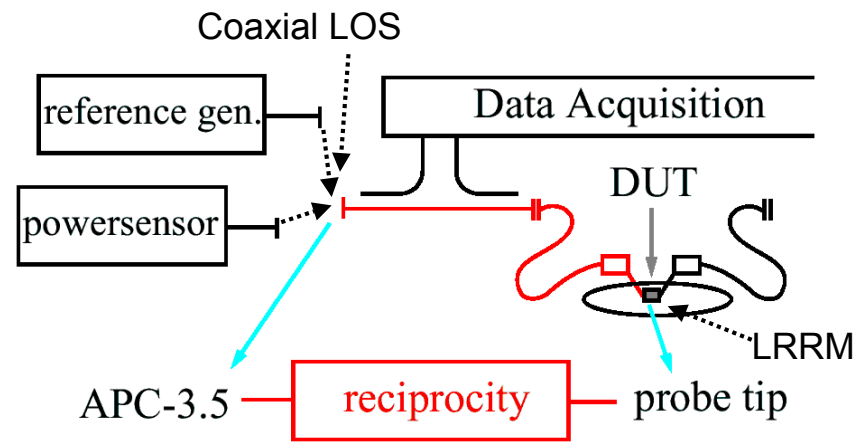

This cannot be done for an on wafer calibration since both the harmonic phase reference generator and the power sensor have a coaxial output connector.

The solution to this problem is based on the use of the reciprocity principle between the probe tip and the "generator input connector" of the test-set.

The harmonic phase reference generator and the power sensor are connected to this coaxial input port and the final measured characteristic can be transformed to the probe tip using the assumption that the test-set is reciprocal. This transformation does require an additional LOS calibration at the "generator input connector".

During all of the above measurements the probe tips are connected to a "line" calibration element.

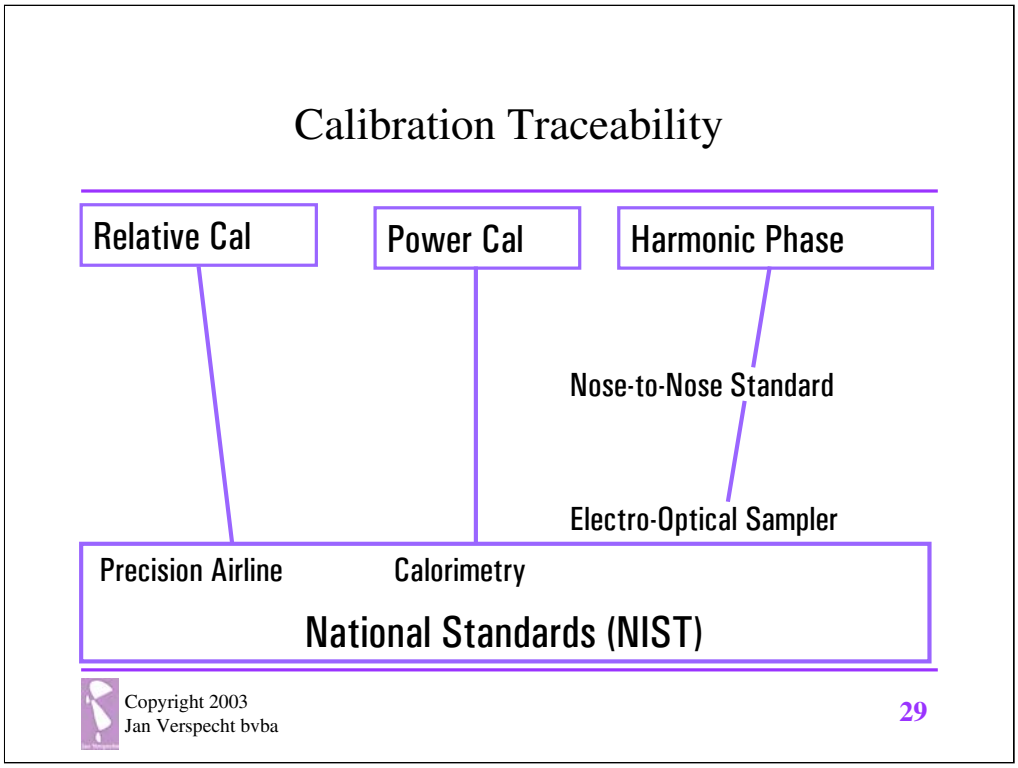

An important aspect of a calibration procedure is its traceability path to metrology grade standards. Each LSNA calibration procedure uses a priori knowledge on the calibration elements. This knowledge is gained through the comparison of the standard elements with higher precision standards. The above slide illustrates the traceability path for the LSNA standards. The relative calibration standards (load, open, short) are traceable to precision airlines with precisely known geometry and material constants which are kept at the calibration elements manufacturer and which are traceable to the National Institute of Standards and Technologies (NIST). The traceability path for the relative calibration elements is identical to the path which is used for classic S-parameter measurements by a commercial vector network analyzer.

The amplitude calibration of the LSNA is done through the use of a power sensor. This power sensor is traceable to a standard power sensor which resides at the lab of the manufacturer of the power sensor. This precision power sensor is traceable to calorimetric measurements performed at the NIST.

The harmonic phase standard (or phase reference generator) of the LSNA is regularly measured by a sampling oscilloscope. This sampling oscilloscope is first calibrated with the "nose-to-nose" calibration procedure. For the moment there is not yet a traceability path to a standard which resides at the NIST.

Important progress is being made to establish such a traceability path. The nose-to-nose calibration procedure was thoroughly studied at the NIST. Recently D. F. Williams and P. Hale of the NIST were able to compare the phase characteristic of the nose-to-nose measurement with the phase characteristic of a calibrated broadband (110 GHz) electro-optic sampling set-up. This electro-optic sampling set-up will probably provide NIST traceability for harmonic phase measurements in the near future.

Characterization of the Harmonic Phase Reference Generator

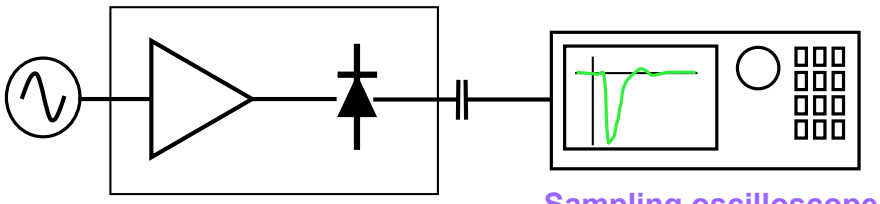

Harmonic Phase Reference generator

Sampling oscilloscope

In what follows we explain the harmonic phase reference procedure of the LSNA, as it is presently in use.

The harmonic phase reference generator is characterized by a broadband sampling oscilloscope. A discrete Fourier transformation returns the phase relationship between all of the relevant harmonics (up to 50GHz).

Note that the harmonic phase reference generator needs to be characterized across a whole range of fundamental frequencies with enough resolution to allow interpolation. For our present generator we cover one octave of fundamental frequencies, from 600MHz up to 1200MHz.

The main components of the harmonic phase reference generator are a power amplifier, a step recovery diode and a pulse sharpening “nonlinear transmission line” (together with cables and padding attenuators).

Sampling Oscilloscope Characterization: Nose-to-Nose Calibration Procedure

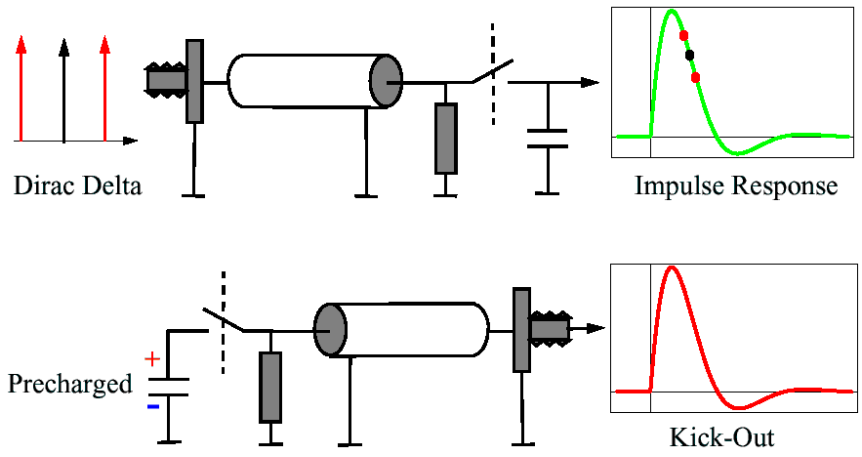

The accuracy of the harmonic phase reference generator characterization is determined by the accuracy of the sampling oscilloscope.

The sampling oscilloscope is characterized by the so-called “nose-to-nose” calibration procedure, which was invented by Ken Rush (Agilent Technologies, Colorado Springs, USA) in 1989.

The basic principle is that each sampler can also be used as a pulse generator. This pulse occurs when an offset voltage is applied to the hold capacitors of the sampler. One can show that this “kick-out” pulse is a very good scaled approximation of the oscilloscope’s “impulse response”.

Nose-to-Nose Measurement

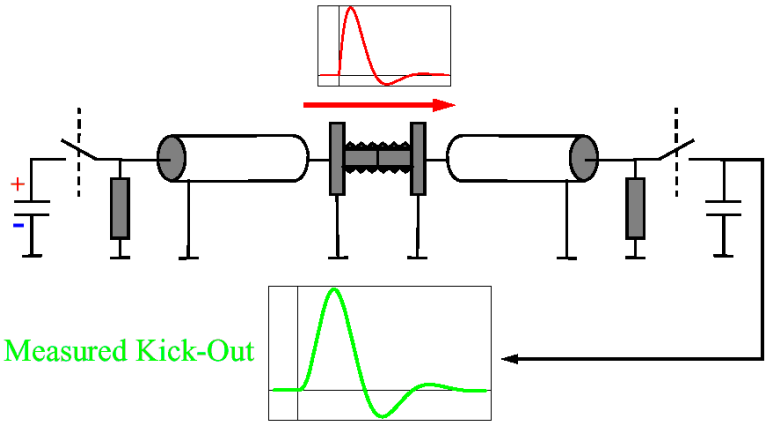

During a nose-to-nose measurement two oscilloscope inputs are connected together and one oscilloscope is measuring the kick-out pulse generated by the other oscilloscope.

Supposing that both oscilloscopes are identical, the resulting waveform is the convolution of the scope's impulse response with the scope's kick-out pulse. Knowing that both are proportional allows to calculate the impulse response. The needed de-convolution is done by taking the square root in the frequency domain.

3 Oscilloscopes are Needed

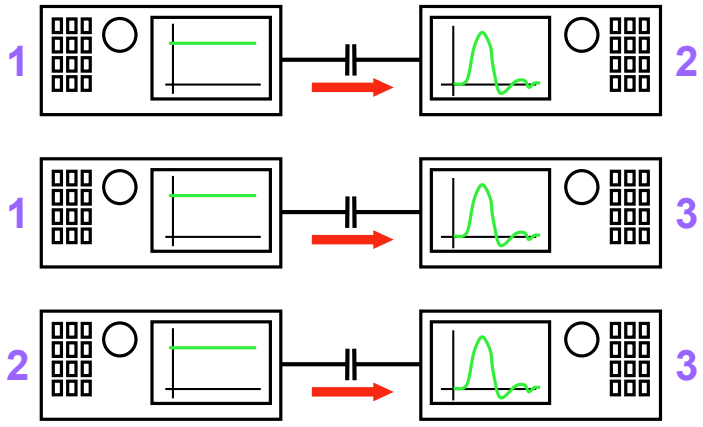

The assumption that the scopes are identical is no longer needed if one performs the nose-to-nose with three oscilloscopes.

Research on the accuracy of the nose-to-nose calibration procedure is performed at the NIST (DeGroot, Hale & al., Boulder, Colorado, USA).

Electro-Optic Sampling* (D. Williams et al., NIST)

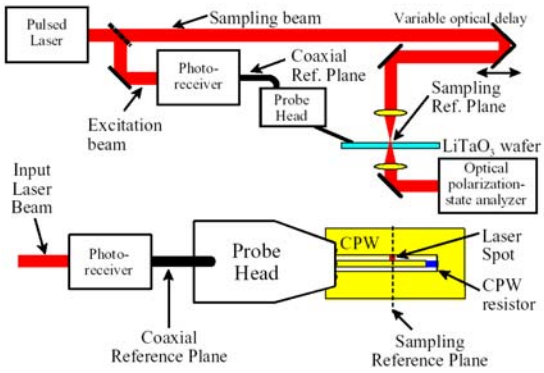

*** The schematic that is shown is "U.S. Government work not subject to copyright."**
D.F. Williams, P.D. Hale, T.S. Clement, and J.M. Morgan, "Calibrating electro-optic sampling systems," ***Int. Microwave Symposium Digest*****, Phoenix, AZ, pp. 1527-1530, May 20-25, 2001.**

The technique of electro-optic sampling as a more accurate standard for the harmonic phase was recently introduced by D. F. Williams of NIST. Such an electro-optic sampling set-up can characterize the small phase error of a nose-to-nose calibration.

The basic principle of an electro-optic sampler is illustrated on the above slide. At the core of the technique is a pulsed laser which generates very short optical pulses. The duration of a pulse of a state-of-the-art pulsed laser is between 100 and 200 femtoseconds. These laser pulses are polarized and travel through a special nonlinear optical crystal which is exposed to the electric field to be measured (sampled). The polarization change of the laser pulses as they travel through the crystal will be proportional to the strength of the electrical field in the crystal during the time the laser pulse was present in the crystal. A precise optical polarization analyzer can then be used to get a read out of the sampled value of the electrical field. It is important that the signal generator is synchronized with the optical pulse.

For more details please check the following reference :

D.F. Williams, P.D. Hale, T.S. Clement, and J.M. Morgan, "Calibrating electro-optic sampling systems," Int. Microwave Symposium Digest, Phoenix, AZ, pp. 1527-1530, May 20-25, 2001.

Outline

- Part I
  - Introduction
  - Instrumentation and Calibration
- Break
  - Coffee and Cookies
- Part II
  - Applications
  - Conclusions

Time for a break.

Outline

- Part I
  - Introduction
  - Instrumentation and Calibration
- Break
  - Coffee and Cookies
- Part II
  - Applications
  - Conclusions

In Part I we introduced the concept of “Large-Signal Network Analysis” and talked about the instrumentation hardware and the calibration procedures.

In Part II we will focus on applications and we will give examples of how the data that is captured by an LSNA experiment can be used.

Part II - Outline

- Waveform Measurements
- Physical Models
- State-Space Models
- Scattering Functions
- Conclusions

Here is a more detailed outline of Part II of this presentation.

First we will show how the acquired data can be used to measure voltage and current time domain waveforms at the terminals of a transistor.

Next we will show that the data can be used for improving physical transistor models.

Then we will shortly talk about the identification of black-box time domain models which are based on the mathematical theory of the state-space functions. These models are called state-space models.

Finally we will present more in depth information on black-box frequency domain models. These are considered as an extension of the theory of the scattering parameters and are called “scattering functions”.

A short conclusion is drawn at the end of the presentation.

Breakdown Current

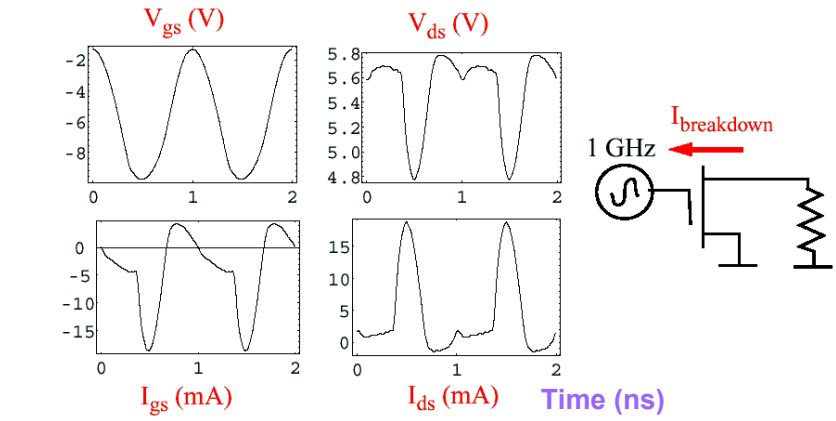

(transistor provided by David Root, Agilent Technologies - MWTC)

As explained previously, the LSNA measures both the amplitude and the phase of all significant harmonics of both the incident and the scattered traveling voltage (pseudo-)waves. Applying an inverse Fourier transform results in corresponding time domain waveforms. The time domain traveling voltage waves can be transformed into a current and a voltage waveform. In the time domain current/voltage visualization mode the LSNA behaves like a broadband oscilloscope having calibrated voltage and current probes. Such information can be very valuable to get a unique insight in e.g. transistor reliability issues, which are often related to hard nonlinear phenomena.

On the above figures we see the voltage and current time domain waveforms as they appear at the gate and drain of a FET transistor. These measurements were performed while applying an excitation signal of 1GHz at the gate. The signal amplitude is increased until we see a so-called breakdown current. It shows up as a negative peak (20mA) for the gate current, and as an equal amplitude positive peak at the drain. We actually witness a breakdown current which flows from the drain towards the gate. This kind of operating condition deteriorates the transistor and is a typical cause of transistor failure.

By our knowledge the above figures show the first measurements ever of breakdown current under large-signal RF excitation.

Forward Gate Current

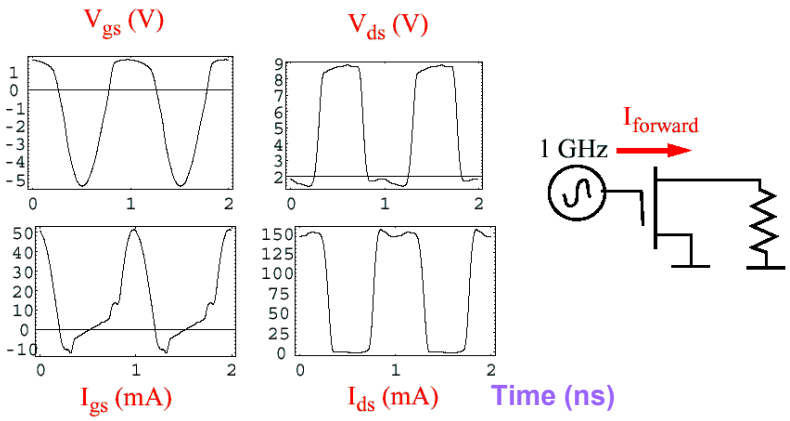

Another similar measurement is shown above.

This time we are biased at a less negative gate voltage then the one used for the breakdown measurements.

We now see that the gate junction is turned on (forward conductance) by the large 1GHz input signal. We see a clipping of the gate voltage (which is behaving like a rectifier), with a positive peak of 50mA in the gate current. The drain current is clipped to 0mA on the low end, and at a value of 150mA at the high end (this occurs during the time the gate is conducting).

Resistive Mixer Schematic

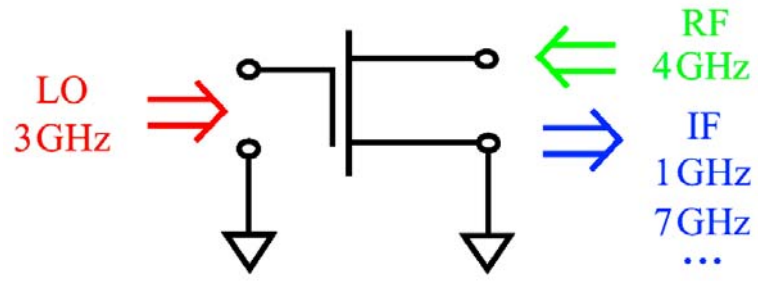

(no drain bias applied)

(transistor provided by Dominique Schreurs, IMEC & KUL-TELEMIC)

Another example is the usage of a HEMT transistor in a resistive mixer configuration.

The schematic of the mixer is illustrated above.

A large local oscillator signal is driving the gate. This causes the drain of the transistor to behave as a time dependent switch. The switch is toggled at the rate of the local oscillator (in our example 3GHz).

Any incident voltage wave at the drain (in our example 4GHz) experiences a fast time varying reflection coefficient (toggling at a 3GHz rate). The voltage wave reflected from the drain will thus be equal to the incident wave multiplied by the time varying reflection coefficient. The scattered wave will contain the mixing products (1GHz and 7Ghz) of the local oscillator and the incident RF signal.

Resistive Mixer: Time Domain Waveforms

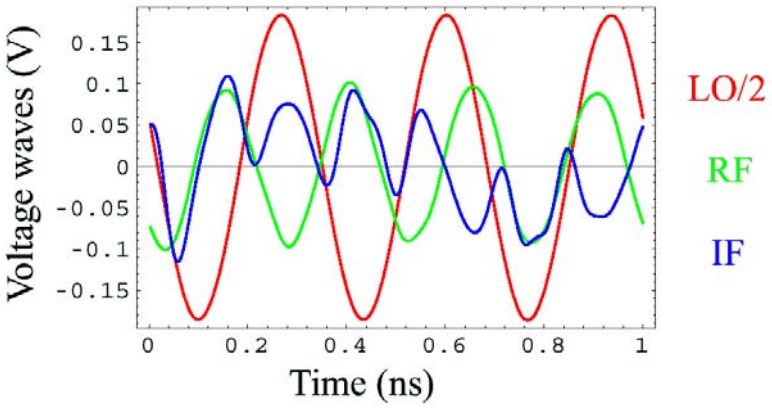

This working principle is nicely demonstrated by looking at the measured time domain representation of the voltage waves.

The figure illustrates how the incident wave (RF) and reflected wave (IF) are in phase or in opposite phase depending on the instantaneous amplitude of the LO. For a high LO the RF experiences a low drain impedance and behaves like a short, corresponding to a reflection coefficient close to -1 (reflection in opposite phase), for a low LO the RF experiences a high drain impedance and behaves like an open, corresponding to a reflection coefficient close to +1 (reflection in phase).

Note that one can clearly distinguish a 1GHz and a 7GHz component in the resulting reflected wave (IF).

High-Speed Digital Signal Integrity

Calibrated Eye Measurement On Wafer (@10GB/sec)

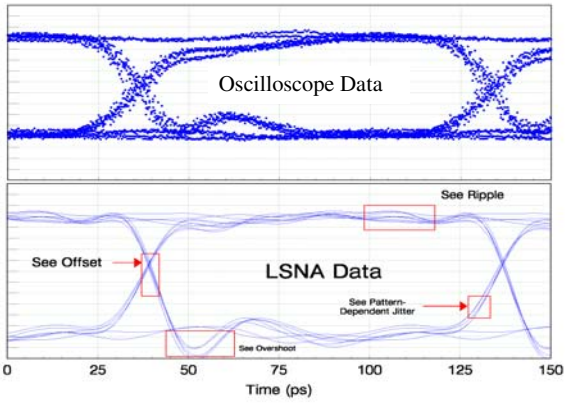

(courtesy of Jonathan Scott, Agilent Technologies)

Another interesting application is the calibrated on wafer measurement of high-speed digital signals. The classic technique for performing such measurements makes use of a microwave oscilloscope. The cables, connectors and probes that are used to connect the oscilloscope to the wafer introduce significant distortions in the measurement of so-called eyediagrams of digital signals. Performing similar measurements with an LSNA results in fully error corrected waveforms all the way up to the tip of the probe. On the slide above one can clearly see that the oscilloscope data lacks certain details like offset and overshoot when compared to the calibrated LSNA data. This is due to dispersion of the oscilloscope cables as well as to the presence of jitter on the timebase of the oscilloscope. These distortions are totally compensated by the LSNA calibration procedure. Although not shown in the picture, the data as measured by the LSNA was much closer to the data generated by the circuit simulator.

Loadpull and Waveform Engineering

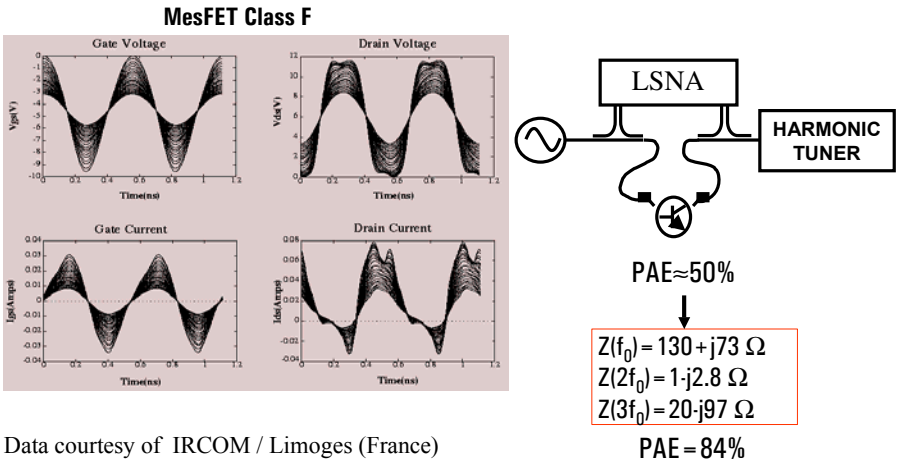

Data courtesy of IRCOM / Limoges (France)

Another application of waveform measurements is power amplifier design by applying "waveform engineering". With waveform engineering one applies different harmonic impedances at the D.U.T. signal ports and one optimizes specific performance parameters like e.g. power-added-efficiency (PAE) by looking at the voltage and current waveforms. Since current and voltage waveforms are not readily available from measurements, the method is usually applied in a simulator. The problem with using simulators is that the accuracy of the final result will depend heavily on the quality of the large-signal transistor model.

Connecting an harmonic tuner to the test-set of the LSNA makes it possible to apply the method in real life, without the need of a simulator or transistor model.

Using the combination of an LSNA with a tuner and using the waveform engineering technique Jean-Michel Nébus et al. could demonstrate an increase of the PAE of a MesFET Class F amplifier from 50% to a record 84%.

For more details please check the following reference.

D. Barataud, F. Blache, A. Mallet, P. P. Bouysse, J.-M. Nébus, J. P. Villotte, J. Obregon, J. Verspecht, P. Auxemery, "Measurement and Control of Current/Voltage Waveforms of Microwave Transistors Using a Harmonic Load-Pull System for the Optimum Design of High Efficiency Power Amplifiers," IEEE Transactions on Instrumentation and Measurement, Vol. 48, No. 4, pp. 835-842, August 1999.

Part II - Outline

- Waveform Measurements
- Physical Models
- State-Space Models
- Scattering Functions
- Conclusions

Next we will show how the LSNA data can be used for improving physical transistor models.

Physical Models

- Represent transistor behavior
- Use electrical circuit schematics
- Contain linear and nonlinear elements such as current sources, capacitors, resistors
- E.g. BSIM3, Chalmers, Materka, Curtice,…

By physical models we refer to electrical circuit schematics containing nonlinear capacitors, voltage controlled current sources, resistors,…

All nonlinear elements are typically defined by means of analytical functions, which are often derived from the physical description of the transistor (geometry, semi-conductor doping profiles,…). These models can have more than 100 parameters which need to be determined.

Examples of such models are BSIM3, Chalmers, Materka,…

Physical Model Improvement

(courtesy of Dr. Dominique Schreurs, IMEC & KUL-TELEMIC)

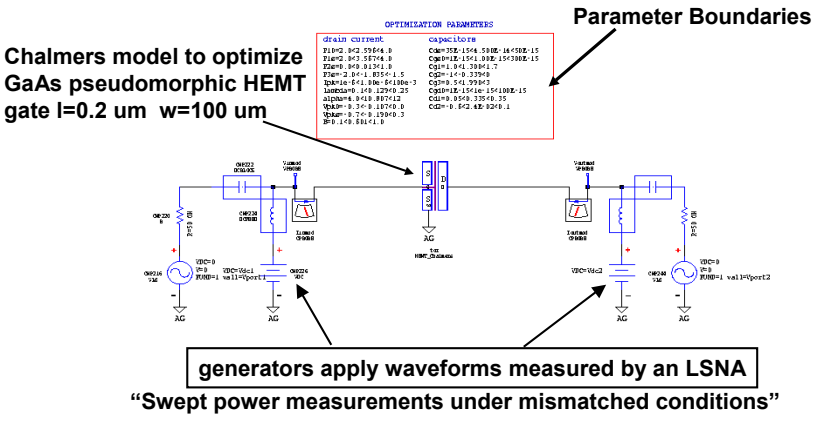

"Swept power measurements under mismatched conditions"

The approach of optimizing existing physical models is pretty straightforward. For our example we use a so-called "Chalmer's model".

First a set of LSNA experiments is performed which covers the operating range of the transistor.

This data is imported into a simulator. The measured incident voltage waves are applied to the model in the simulator.

Using the Built-in Optimizer

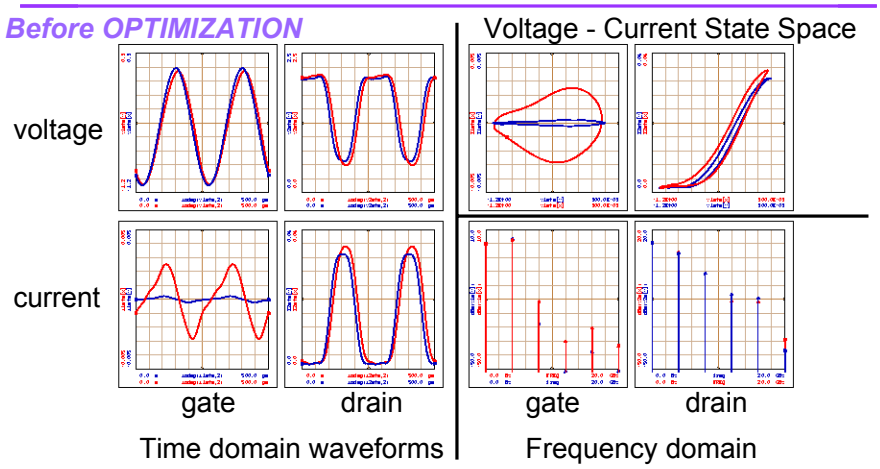

The model parameters are then found by tuning them such that the difference between the measured and modeled scattered voltage waves is minimized.

Note that one can often use built-in optimizers for this purpose.

As with all nonlinear optimizations it is necessary to have reasonable starting values (these can be given by a simplified version of the classical approaches).

The figures above represent one of the modeled and measured gate and drain voltages and currents, and this in the time domain, the frequency domain and in a “current-versus-voltage” representation.

Note especially the large discrepancy between the measured gate current and the one which is calculated by the initial model.

Verification of the Optimized Model

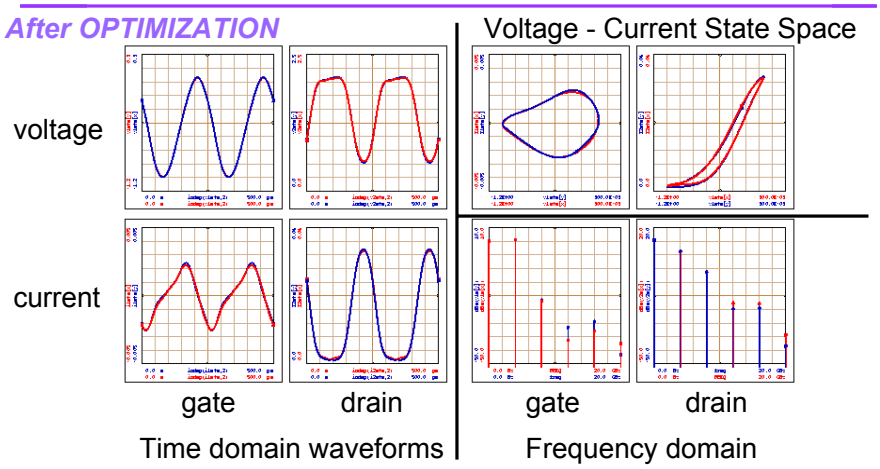

The above figures represent the same data after optimization has taken place to improve the model.

Note the very good correspondence that is achieved. This indicates that the model is accurately representing the large-signal behavior for the applied excitation signals. The optimizer had mainly an effect on the parameters associated with the nonlinear gate capacitance.

Part II - Outline

- Waveform Measurements
- Physical Models
- State-Space Models
- Scattering Functions
- Conclusions

We will now present how the LSNA data is used with state-space modeling techniques.

State Space Function Model

$$I_1 = F_1\left(V_1, V_2, \frac{dV_1}{dt}, \frac{dV_2}{dt}, \frac{dI_1}{dt} \ldots\right)$$

$$I_2 = F_2\left(V_1, V_2, \frac{dV_1}{dt}, \frac{dV_2}{dt}, \frac{dI_1}{dt} \ldots\right)$$

Fit with e.g. artificial neural network or spline
(David Root, John Wood, Dominique Schreurs)

State-space models are black-box time domain models. These kind of models are typically used in physics for describing all kinds of nonlinear dynamical processes. A first microwave transistor model of this kind is the so called Root-model. It is a simple version of the more general "state-space function model". It was originally invented by Dr. David Root. For a Root-model the model parameter extraction is based on bias dependent S-parameter measurements. The connection between state-space model parameter extraction and "large-signal network analyzer" measurements was done by Dr. Dominique Schreurs.

In a state-space function approach, one assumes that the port currents of a device are a general nonlinear function of a limited set of state variables. The state variables are the port voltages, the first and higher order derivatives of the port voltages, and the first and higher order derivatives of the port currents. One can identify the relevant set of state variables and the functions themselves by performing sufficient LSNA experiments and by processing the gathered data.

The state-space models are technology independent and can be applied to all nonlinear microwave circuits as long as they do not contain distributed elements. Examples are single transistors or small RFIC's. As soon as distributed elements are present the set of relevant state-space variables becomes excessively large (in theory an infinite number) and the state-space functions can no longer be practically identified.

Experiment Design:
Crucial to Explore Component Behavior

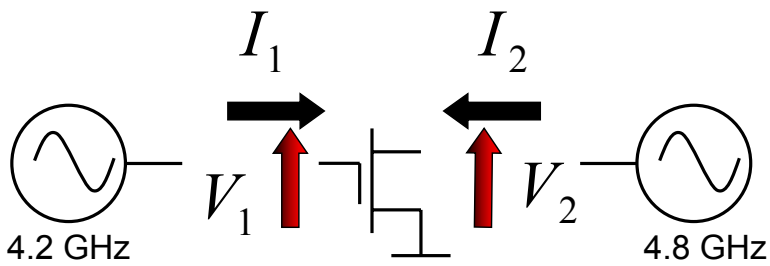

One of the main challenges is the experiment design. In order to have a good fit to the state-space functions it is necessary to have a dense coverage of the state-space over a meaningful range.

An original solution to this was used by Dr. Schreurs. She applied an excitation to the gate and the drain of the transistor at a different frequency, namely 4.2GHz and 4.8GHz. Note that both frequencies are integer multiples of 600MHz, which implies that a single frequency grid of 600MHz is sufficient for the LSNA data acquisition.

State Space Coverage through Proper Experiment Design

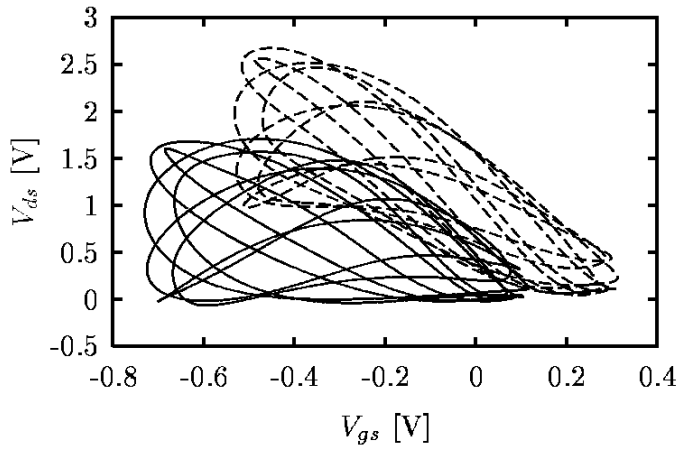

This figure illustrates the resulting coverage of the state-space corresponding to two measurements (2 different bias settings are applied).

The 2-tone experiment allows a dense coverage of the state-space over a meaningful range.

It might be interesting to note that the 2-tone technique was actually invented several decades ago by mechanical engineers dealing with the characterization of nonlinear mechanical structures.

Part II - Outline

- Waveform Measurements
- Physical Models
- State-Space Models
- Scattering Functions
- Conclusions

As a final application we will talk about how the LSNA can be used to extract “scattering function” models.

When to use Scattering Functions?

Scattering functions are

- Black-box frequency domain models,
- Directly derived from large-signal measurements.

Scattering functions are used

- With new less understood technology
- When there is a difficult de-embedding problem
- When there are multiple transistors in the circuit
- When the component has distributed characteristics

The “scattering functions” modeling approach is a “black-box frequency domain” model.

Such models can be used when one has a hard time to build physical models or state-space function models.

This is often the case for new, less understood technology, for complex de-embedding problems, for multi-transistor circuits (e.g. large RFIC’s and system amplifiers), or for a DUT which has distributed characteristics.

The idea is to do a set of frequency domain measurements which covers a specific application (e.g. a narrowband 1.9GHz power amplifier). Based upon the acquired data one can then fit so-called “scattering functions”. These are the multi-dimensional complex functions which describe the relationship between the incident and the scattered spectral components.

Theoretical Concepts

Scattering Functions → Quantities are Waves

for

Nonlinear Behavioral Modeling → Functional Relationship

in the

Frequency Domain → Input and Output are Discrete Tone Signals

We will now explain the theoretical concepts of the scattering functions.

The word “scattering” in “scattering functions” refers to the fact that we are working with traveling wave quantities as it is the case with S-parameters. Note that, by convention, we use traveling voltage waves.

In general we will be working with general functional relationships between the wave quantities. This is very different from S-parameters which can only describe a linear relationship.

The scattering functions approach assumes the presence of discrete tone signals (multisines) for the incident as well as for the scattered waves.

Quantities are Traveling Voltage Waves

$$\begin{pmatrix} V \\ I \end{pmatrix} \rightarrow \begin{pmatrix} A^{(Z)} \\ B^{(Z)} \end{pmatrix} = \begin{pmatrix} \frac{V + ZI}{2} \\ \frac{V - ZI}{2} \end{pmatrix}$$

Default value of Z = 50 Ohm (classic S-parameters)

The “traveling voltage waves” are defined as it is the case for classic S-parameters. They are linear combinations of the signal port voltage and current. The default value of the characteristic impedance that is used is 50 Ohms. For certain applications, however, the choice of another value may be more practical. An example are power transistor applications where it may be simpler to use a value which comes close to the output impedance of the transistor.

Note that the waves are defined based upon a pure mathematical transformation of the signal port voltage and current and that they are not associated with a physical wave transmission structure. Therefore the wave quantities are more accurately called “pseudo-waves” (R. Marks and D. Williams, “A general waveguide circuit theory,” J. Res. Natl. Inst. Stand. Technol., vol. 97, pp. 533-562, Sept./Oct. 1992).

Scattering Functions Describe:

- Compression characteristic
- Spectral regrowth
- AM-PM
- PAE
- Harmonic Distortion
- Fundamental loadpull behavior
- Harmonic loadpull behavior
- Time domain voltage & current
- Influence of bias can be included

The black-box frequency domain models based on the scattering functions can accurately describe many large-signal effects.

E.g. compression characteristics, spectral regrowth (ACPR), AM-PM conversion, power-added-efficiency, harmonic distortion, fundamental and harmonic loadpull behavior, time domain voltage and current waveforms, self biasing effects….

Notation - Graphical Illustration

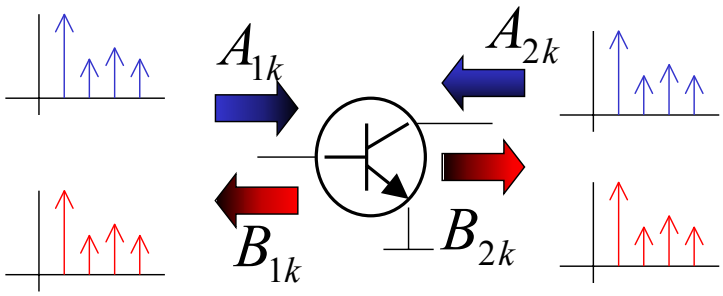

$$B_{1k} = F_{1k}(A_{11}, A_{12}, ..., A_{21}, A_{22}, ...)$$
$$B_{2k} = F_{2k}(A_{11}, A_{12}, ..., A_{21}, A_{22}, ...)$$

We will use the following notations.

The incident waves are represented by a capital A and the scattered waves by a capital B. The first subscript refers to the signal port and the second subscript refers to the "harmonic index". Note that an harmonic index of 1 refers to the fundamental component. In general we are looking for the mathematical functions F which correlate the input spectral components A_{1k} and A_{2k} with the output spectral components B_{1k} and B_{2k}.

Phase Normalization

- "Phase normalized" quantities are used
- Defines unambiguous phase for harmonics
- Large-signal A_{11} is the phase reference (most useful for many applications)

In order to simplify the mathematics it is important to use "phase normalized" quantities. This is especially useful since harmonic frequencies are present. The "phase normalization" makes it possible to define the phase of an harmonic in a unique way. For the rest of this presentation we will always use A_{11} (the incident fundamental) as our phase reference component. This is especially useful for power transistor and power amplifier applications, where A_{11} is the dominant large-signal input component.

Phase Normalization: Mathematics

- We define a reference phasor: $P = e^{j\varphi(A_{11})}$
- We define phase normalized quantities:

$$A_{mk}^{N} = A_{mk} P^{-k} \qquad B_{mk}^{N} = B_{mk} P^{-k}$$

- Special case: $A_{11}^{N} = \left| A_{11} \right|$

The mathematics of the phase normalization is pretty simple. We define a component P which has a phase equal to the phase of A_{11}, but which has a unity length. The normalized quantities, denoted by the superscript N, are then calculated by multiplying the raw quantities by the reciprocal of P raised to the power k, which corresponds to the harmonic index of that component.

Note that the phase normalized A_{11}^{N} is a special case and is equal to a positive real number equal to the amplitude of A_{11}.

Harmonic Superposition Principle

- In general superposition cannot be used to describe the functional relationship between the spectral components

$$F(A + A') \neq F(A) + F(A')$$

- The superposition principle can be used for relatively small components (e.g. harmonics)

In general we are not working with linear relationships and the superposition principle is not valid. In many practical cases (e.g. power amplifiers) there is only one dominant large-signal input component present (A_{11}) where as all other input components (the harmonic frequency components) are relatively small. In that case we will be able to use the superposition principle for the relatively small input components. This is called the harmonic superposition principle.

Harmonic Superposition: Illustration

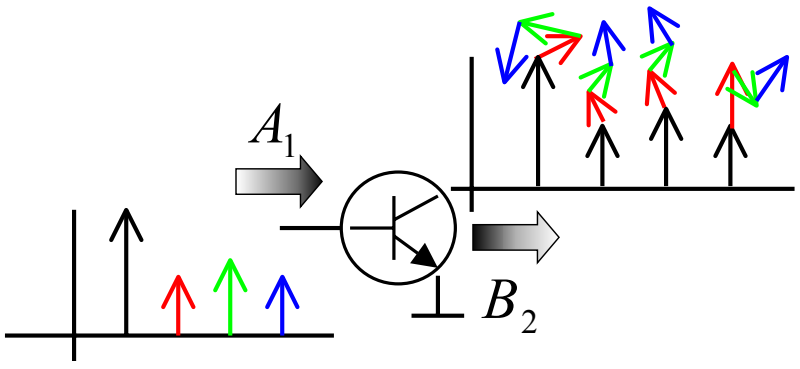

The "harmonic superposition" principle is graphically illustrated above. In order to keep the graph simple we only consider here the presence of an A_1 and B_2 and we neglect the presence of A_2 and B_1. First let us consider the case where only A_{11} is different from zero. The input spectrum A_1 and output spectrum B_2 corresponding to this case are indicated by black arrows. Note the presence of significant harmonic components for B_2. Now leave the A_{11} excitation the same and add a relatively small A_{12} component (second harmonic at the input). This will result in a deviation of the output spectrum B_2, indicated by the red arrows. The same holds of course for a third (green) and a fourth (blue) harmonic. The "harmonic superposition" principle holds when the overall deviation of the output spectrum B_2 is the superposition of all individual deviations. This conjecture was experimentally verified and appeared to be true for all practical power amplifier design cases, whatever the class of the amplifier. The harmonic superposition principle is the key to a practical implementation of the scattering functions.

Basic Mathematical Equation

$$B_{mk}^{N} = \sum_{nh} S_{mknh}(A_{11}^{N})A_{nh}^{N} + \sum_{nh} S'_{mknh}(A_{11}^{N})A_{nh}^{N*}$$

- A_{11} assumed to be the only large-signal component
- Superposition assumed to be valid for other A_{nh}
- The notation A* means the complex conjugate of A
- S and S' are called the scattering functions
- Note that $S'_{mk11} = 0$

The harmonic superposition principle leads to a very simple mathematical formulation which is shown above. The phase normalized B^N waves are the output quantities. They are written as a linear combination of the phase normalized A^N waves, the input quantities, and their conjugates. Note that the resulting expression is linear in all components A_{nh} and their conjugates, except for A_{11} which is assumed to be the only large-signal component for which the superposition principle does not hold. This is an assumption which was experimentally verified and found to be valid in all practical cases of power amplifier design. Since $A_{11}{}^N$ is a strictly positive real number one can define S'_{mk11} equal to zero without compromising the structure of the equation. The functions S and S', which have both an amplitude and a phase, are called "scattering functions". They are general nonlinear functions of $A_{11}{}^N$ but they are independent of the components for which the superposition principle holds. As such they are a natural extension of S-parameters. Note that each S-function is denoted by 4 subscripts: the first two to denote the port and harmonic index of the B component, and the latter two to describe the port and harmonic index of the A component.

The scattering functions have some unique features when compared to S-parameters. First of all they relate input and output spectral components which have different frequencies. They can describe e.g. how A_{13}, the third harmonic of the incident wave, will contribute to a change in B_{22}, the second harmonic at port 2. This corresponds to the concept of the "conversion matrix" well known by mixer designers. A characteristic which appears to be counter-intuitive to many people is the existence of S' which is the coefficient associated with the conjugate of the A^N waves. In a nutshell, S' describes the fact that the ratio between the scattered B^N and incident A^N waves depends on the phase of the A components relative to A_{11}.

Applications: Compression and AM-PM conversion

- Only considering B_{21} and A_{11} results in

$$B_{21}^N = S_{2111}(A_{11}^N)A_{11}^N$$

- This can be rewritten as

$$S_{2111}(|A_{11}|) = \frac{B_{21}}{A_{11}}$$

- $S_{2111}(|A_{11}|)$ represents the compression and AM-PM conversion characteristic

The scattering functions formalism covers many applications. The S_{2111} function can be interpreted as the compression and AM-PM conversion characteristic of a device. Note that defining the resulting compression and AM-PM conversion characteristic this way implicitly assumes that it is independent from harmonic components and from the fundamental component incident to port 2. Classic compression and AM-PM characteristics are usually measured on systems having imperfect matching characteristics. As a result classic measurements of these characteristics differ from measurement system to measurement system because of the presence of different matching characteristics. The S_{2111} numbers returned by a scattering functions measurement set-up compensate for the non-ideal instrument port match. This is actually similar to what happens with a vector network analyzer. Although the port match of two VNA's may significantly differ, the S-parameters returned are not affected. As such the measured scattering functions are true device characteristics, not disturbed by instrument imperfections.

Large-Signal Input Match

- Only considering B_{11} and A_{11} results in

$$B_{11}^N = S_{1111}(A_{11}^N)A_{11}^N$$

- This can be rewritten as

$$S_{1111}(|A_{11}|) = \frac{B_{11}}{A_{11}}$$

- $S_{1111}(|A_{11}|)$ represents the large-signal input reflection coefficient

In a similar way the S_{1111} function can be interpreted as the large-signal input reflection coefficient.

Hot S_{22}

- Considering B_{21}, A_{21} and A_{11} results in

$$B_{21}^{N} = S_{2111}(A_{11}^{N})A_{11}^{N} + S_{2121}(A_{11}^{N})A_{21}^{N} + S'_{2121}(A_{11}^{N})A_{21}^{N*}$$

- Multiplying both sides with P results in

$$B_{21} = S_{2111}(|A_{11}|)A_{11} + S_{2121}(|A_{11}|)A_{21} + S'_{2121}(|A_{11}^{N}|)P^{2}A_{21}^{*}$$

- The combination of S_{2121} and S'_{2121} are a scientifically sound format for "Hot S_{22}"

Looking at S_{2121} and S'_{2121} results in an original and scientifically sound definition of "Hot S_{22}". It is important to understand that "Hot S_{22}" behavior can only be tackled in a scientifically sound way by using the combination of S_{2121} and S'_{2121}. By our knowledge this is an original result. Classic "Hot S_{22}" approaches completely ignore the existence of the S'_{2121} component. When written in quantities which are not phase normalized we see the appearance of P^2.

Measurement Example

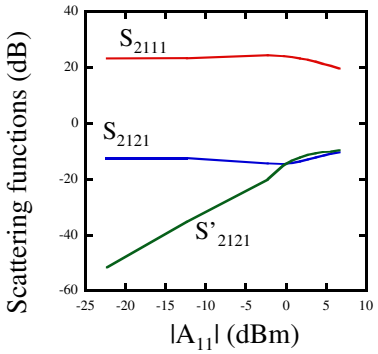

- Note that the amplitude of S'_{2121} becomes arbitrary small for $|A_{11}|$ going to zero

Above we show a practical measurement of the amplitude of S_{2111}, S_{2121} and S'_{2121} as a function of the amplitude of A_{11}.

We clearly see the compression characteristic of S_{2111}. Especially interesting is the analysis of the behavior of the scattering functions for small amplitudes of A_{11}. For small A_{11} amplitudes S_{2111} and S_{2121} are constants, equal to the classic S-parameters s_{21} and s_{22}. S'_{2121} on the contrary becomes arbitrarily small for small amplitudes of A_{11}. This illustrates the fact that the component S'_{2121} is only visible under large-signal (nonlinear) operating conditions. Note that the amplitude of S'_{2121} becomes significant at relatively low levels of compression. As such problems can be expected with classic "Hot S_{22}" approaches since they completely neglect the existence of this component.

Harmonic Distortion Analysis

- Only considering A_{11} and B_{2k} one can calculate the harmonic distortion as a function of $|A_{11}|$

$$B_{21} = S_{2111}(|A_{11}|)A_{11}$$
$$B_{22} = S_{2211}(|A_{11}|)A_{11}P$$
$$B_{23} = S_{2311}(|A_{11}|)A_{11}P^2$$

The scattering functions contain all the information that is needed to calculate the phase and amplitude of the harmonics as a function of the input amplitude. They can as such be used for harmonic distortion analysis.

Harmonic Loadpull Behavior

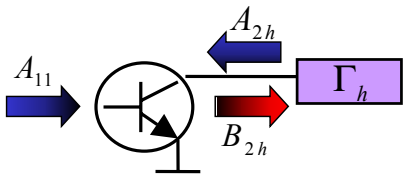

$$B_{2k}^N = \sum_h S_{2k2h}(A_{11}^N)A_{2h}^N + \sum_h S'_{2k2h}(A_{11}^N)A_{2h}^{N*}$$

$$A_{2h}^N = \Gamma_h B_{2h}^N$$

- Solve the set of equations
  (linear in the real and imaginary parts of A_{2h} and B_{2h})

An important application is the prediction of fundamental and harmonic loadpull behavior. In this case we want to predict the B_{2h} waves (particularly B_{21}) as a function of the matching conditions at the output, both for the fundamental and the harmonics. This can be achieved by solving the set of equations represented above. The first set of equations represent the scattering functions, the second set mathematically represents the matching conditions. Note that the set of equations is linear when one considers the real and imaginary parts of A_{2h} as separate variables and is as such easy to solve.

New Stability Circles for Multiplier Design

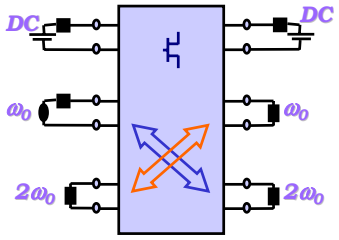

Research performed by
Prof. Giorgio Leuzzi
(Universita dell'Aquila, Italy)

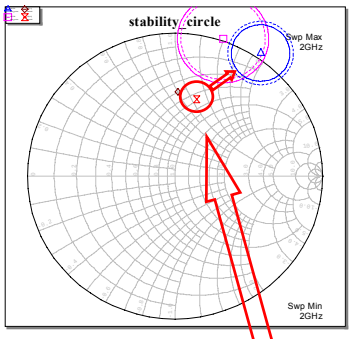

Stability is not ensured

A recent application is the definition of large-signal stability circles. They are especially useful for the stability analysis encountered with the design of frequency multipliers. This research is performed by Prof. Giorgio Leuzzi of the Universita dell'Aquila (Italy). In this research work it is shown that the scattering functions are very closely related to the Jabobian as it is used in harmonic balance simulators.

Practical Measurement: Experiment Design Concept

- Simple example: S_{2111}, S_{2121} and S'_{2121}

$$B_{21}^{N} = S_{2111}(A_{11}^{N})A_{11}^{N} + S_{2121}(A_{11}^{N})A_{21}^{N} + S'_{2121}(A_{11}^{N})A_{21}^{N*}$$

- Perform 3 independent experiments

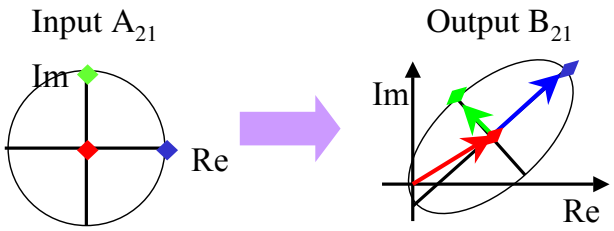

The experiment design concept to extract the actual values of the scattering functions is pretty straightforward. Assume that we want to know S_{2111}, S_{2121} and S'_{2121} for a particular amplitude of A_{11}. We apply the particular A_{11} amplitude and we keep it constant during the rest of the experiment. First we do not apply any other incident wave besides A_{11} (this experiment is represented by the red square). This results in the knowledge of S_{2111}. Next we perform two independent experiments, one applying an A_{21} with a zero phase and one applying an A_{21} with a 90 degree phase (corresponding to the blue and respectively green square). Having those two additional measurements we have sufficient information to calculate S_{2121} and S'_{2121}.

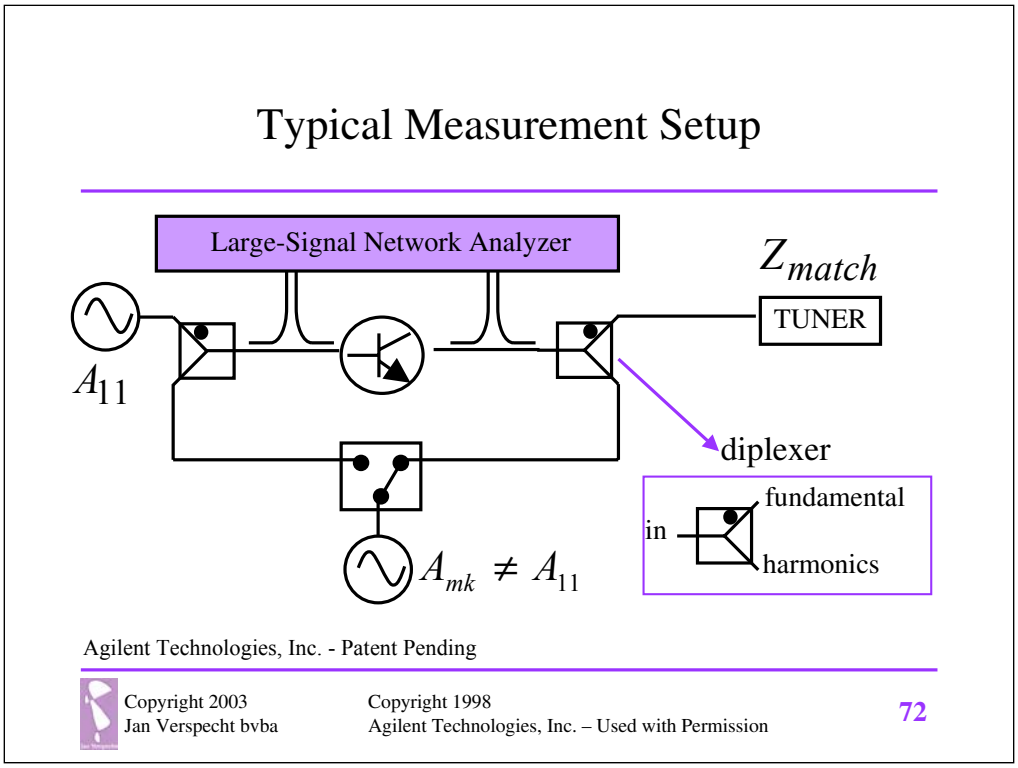

A typical measurement setup is shown above. A Large-Signal Network Analyzer measures all relevant A_{mk} and B_{mk} components. One synthesizer (typically used in combination with a power amplifier) is used for the generation of the A_{11} component. A second synthesizer, combined with a switch, is used for the generation of the harmonic "small signal" components A_{mk}. The fundamental component A_{21} is often generated by using a tuner. The diplexers are there to decouple the fundamental and the harmonic behavior. Note that there is a patent pending with Agilent Technologies related to this technique.

Measurement Example

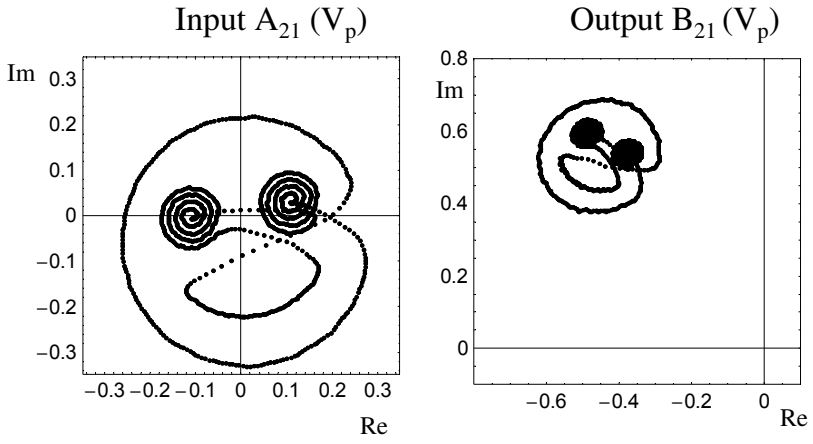

Although 3 measurements are theoretically sufficient to extract the scattering functions one usually performs many more measurements in combination with a linear regression technique. A practical example of such a set of experiments is shown above ☺. The presence of redundancy in the measurement set offers many possibilities in the framework of system identification (gathering information on noise errors and residual model errors).

Link to Harmonic Balance Simulators

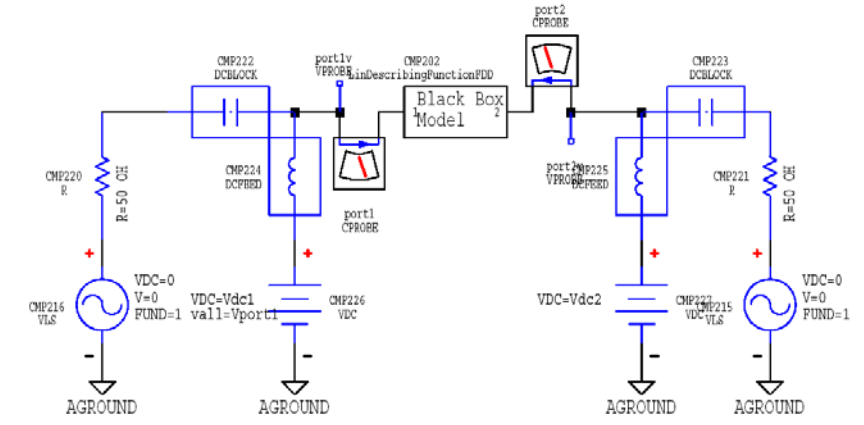

The scattering functions can easily be linked to harmonic balance simulators. In fact their mathematical structure fits the harmonic balance simulator like a glove. This results in memory efficient and fast simulations. Model accuracy is ensured by the fact that the scattering functions are directly derived from measurements. The accuracy statement holds as far as the device-under-test is stimulated under conditions for which the assumed harmonic superposition principle holds.

Simulated Model versus Measurements

Power Transistor Waveforms

Gate Voltage

Drain Voltage

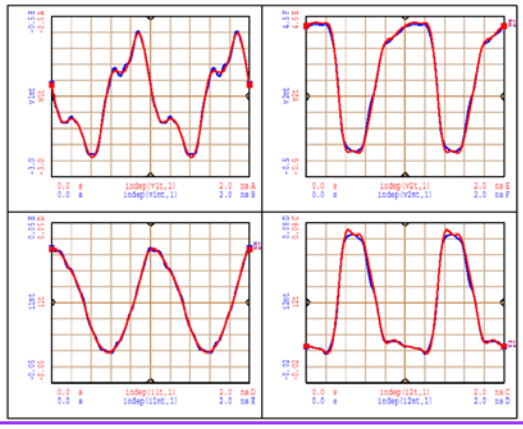

Gate Current

Drain Current

The above graph represents a comparison between the measured and modelled (by means of the scattering functions) time domain current and voltage waveforms at the terminals of a power transistor under loadpull conditions. Note that the loadpull condition was arbitrarily chosen and was not part of the experiment set to extract the scattering functions. As one can see the correspondence is striking and should clearly be sufficient for practical power amplifier design. Note that the modelled waveforms were calculated by putting the scattering functions in an harmonic balance simulator as shown on the previous slide.

Scattering Functions with Modulation

1.9 GHz RFIC (CDMA)

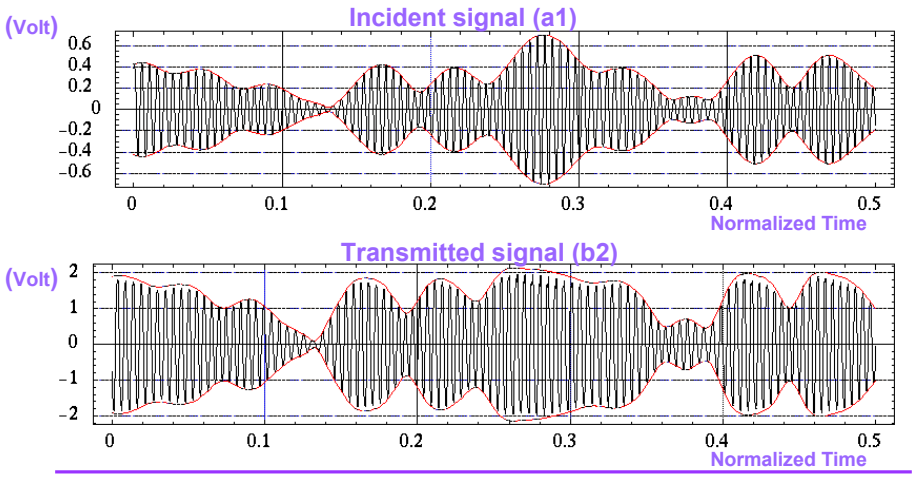

All previously shown modeling techniques dealt with "single frequency grid" measurements. Finally we will demonstrate black-box model extraction based upon modulated measurements.

First, let us take a look at the kind of data provided by these measurements.

The figures above represent the incident and transmitted time domain signals as they were measured at the signal ports of a 1.9GHz RFIC amplifier.

The incident signal has characteristics similar to a CDMA signal.

The transmitted signal clearly suffers from compression and harmonic distortions whenever the input amplitude is high.

Dynamic Harmonic Distortion: Transmitted Signal

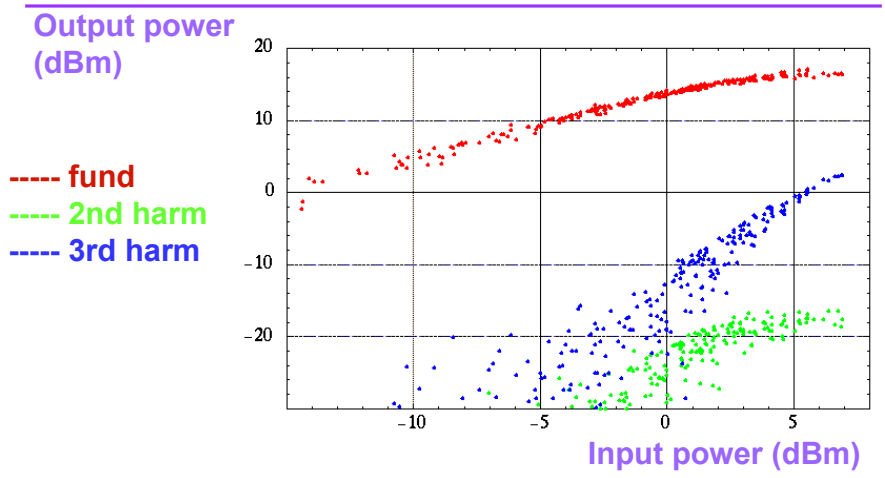

Another way of visualizing this behavior is a so-called “dynamic harmonic distortion” plot.

This is interpreted in exact the same way as a classical harmonic distortion plot, but now the input amplitude does not change step-by-step but changes very fast throughout the modulation period.

The transfer characteristic of the fundamental clearly shows the typical compression effect.

Note that the data also contains the phase information, both for the fundamental and the harmonics. These phase characteristics are not shown in the graphs.

Dynamic Harmonic Distortion: Reflected Signal

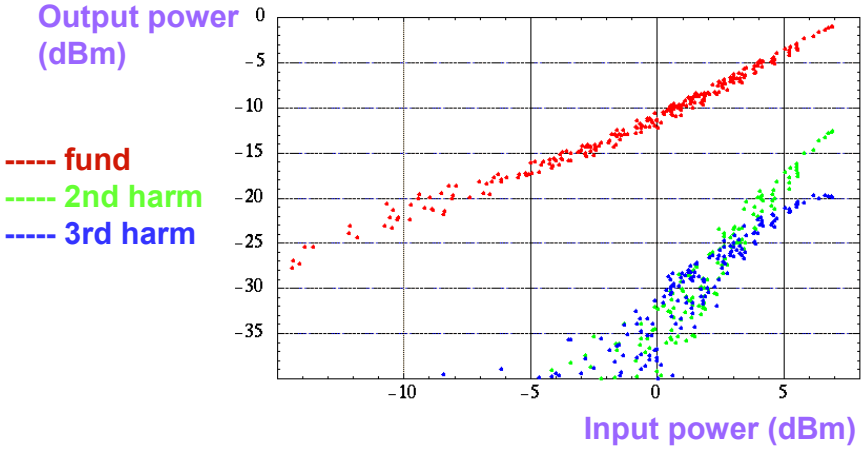

The LSNA can also measure a similar dynamic harmonic distortion plot for the B-wave reflected at the input.

Note that we now have an expansive characteristic for the fundamental. This implies that the input match is worse for higher amplitudes.

This effect can be a significant cause of spectral regrowth when it is combined with an imperfect matching condition of the previous amplifier or signal generator stage. To our knowledge this effect is often, if not always, neglected by designers.

Emulate CDMA Statistics using many Periodic Pseudo-Random Sequences

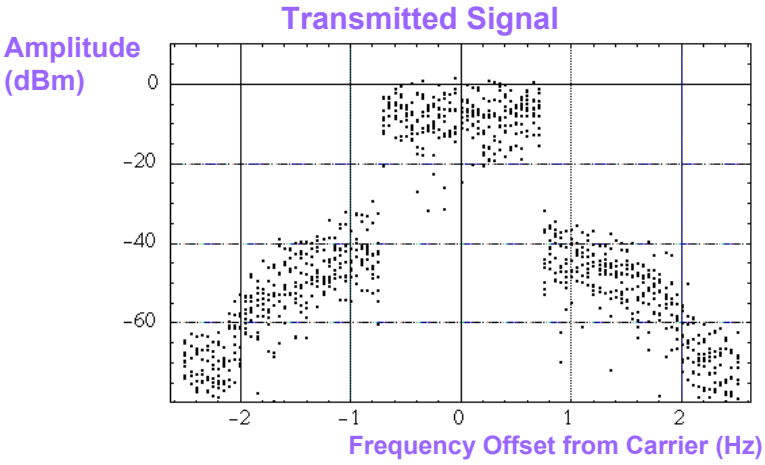

The goal is to extract behavioral models that can describe the kinds of behavior shown in the previous slides (compression, expansion, harmonics,…) under realistic operating conditions, including large-signal modulation.

E.g. if one wants to extract a model which is valid under a CDMA excitation signal it is important that the experiments performed have statistical characteristics similar to CDMA (especially the probability density function of the amplitude).

These statistics can not be emulated very well by one periodically modulated input signal.

The correct statistics are achieved by applying many different periodic pseudo-random sequences.

This is illustrated on the above graphic.

Note the occurrence of spectral re-growth in this set of measurements.

Apply Fitting Technique

- For our example we use a piece wise polynomial (3rd order)

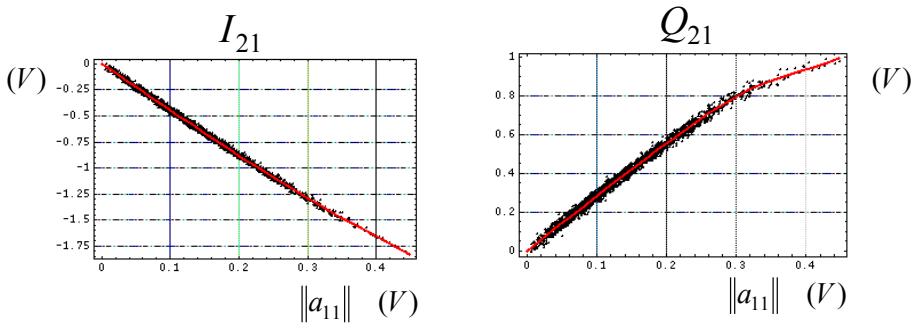

The acquired data can then be used to extract a model.

If one assumes that the behavior of the component is static with respect to the modulated carrier (no memory effects), one can use the same describing function approach as before in order to describe the fundamental as well as harmonic output signals, and this for both the transmitted and the reflected waves.

For the example shown above, a piece wise polynomial of 3rd order is used in order to fit the real and imaginary part of the describing function associated with the transmitted fundamental.

Model Verification - Spectral Regrowth

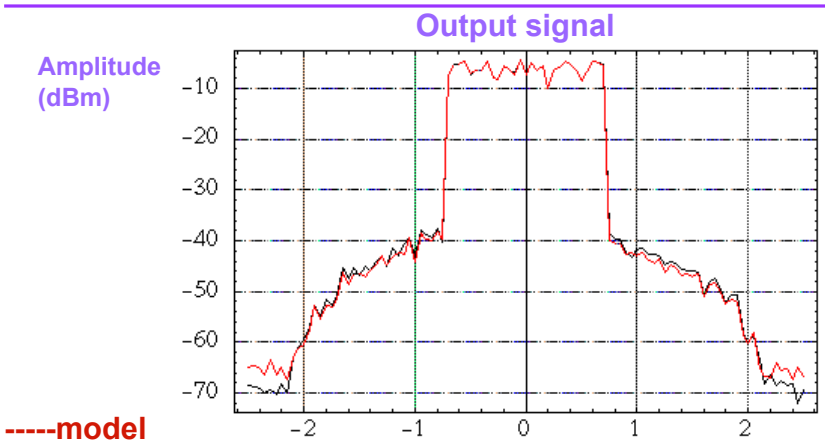

This plot shows an overlay of the measured and modeled spectral re-growth. As one can see the correspondence is very good.

Part II - Outline

- Waveform Measurements
- Physical Models
- State-Space Models
- Black-Box Frequency Domain Models
- Conclusions

As a last part of the presentation, here are the conclusions.

Conclusions

- The dream of accurate and complete large-signal characterization of components under realistic operating conditions is made real
- The only limit to the scope of applications is the imagination of the R&D people who have access to this measurement capability

The dream of accurate and complete large-signal characterization of components under realistic operating conditions is made real.

The only limit to the scope of applications is the imagination of the R&D people who have access to this measurement capability.

"Jan Verspecht bvba" Coordinates

- URL: http://www.janverspecht.com
- email: info@janverspecht.com
- fax: 32-52-31.27.85
- phone: 32-479-85.59.39
- address: Jan Verspecht bvba
  Gertrudeveld 15
  B-1840 Londerzeel
  Belgium

"Jan Verspecht bvba" offers educational, consulting and intellectual property services related to "Large-Signal Network Analysis".

Contact us in case you need any help on LSNA related issues.

Reference Papers

"Jan Verspecht bvba" publications database

Many papers authored or co-authored by Jan Verspecht are available at the following URL: http://www.janverspecht.com

Signal Representations

R. Marks and D. Williams, "A general waveguide circuit theory," Journal of Research of the National Institute of Standards and Technologies, vol. 97, pp. 533-562, Sept./Oct. 1992.

Large-Signal Network Analyzer Hardware

Jan Verspecht, "Calibration of a Measurement System for High-Frequency Nonlinear Devices," Doctoral Dissertation – Vrije Universiteit Brussel, Belgium, November 1995.

Large-Signal Network Analyzer Calibration

Jan Verspecht, Peter Debie, Alain Barel, Luc Martens,"Accurate On Wafer Measurement of Phase and Amplitude of the Spectral Components of Incident and Scattered Voltage Waves at the Signal Ports of a Nonlinear Microwave Device," Conference Record of the IEEE Microwave Theory and Techniques Symposium 1995, pp. 1029-1032, USA, May 1995.

Kate A. Remley, "The Impact of Internal Sampling Circuitry on the Phase Error of the Nose-to-Nose Oscilloscope Calibration," NIST Technical Note 1528, August 2003.

Jan Verspecht, "Broadband Sampling Oscilloscope Characterization with the 'Nose-to-Nose' Calibration Procedure: a Theoretical and Practical Analysis," IEEE Transactions on Instrumentation and Measurement, Vol. 44, No. 6, pp. 991-997, December 1995.

D.F. Williams, P.D. Hale, T.S. Clement, and J.M. Morgan, "Calibrating electro-optic sampling systems," Int. Microwave Symposium Digest, Phoenix, AZ, pp. 1527-1530, May 20-25, 2001.

Waveform Measurements

Jan Verspecht, Dominique Schreurs, "Measuring Transistor Dynamic Loadlines and Breakdown Currents under Large-Signal High-Frequency Operating Conditions," 1998 IEEE MTT-S International Microwave Symposium Digest, Vol. 3, pp. 1495-1498, USA, June 1998.

Jonathan B. Scott, Jan Verspecht, B. Behnia, Marc Vanden Bossche, Alex Cognata, Frans Verbeyst, M. L. Thorn, D. R. Scherrer, "Enhanced on-wafer time-domain waveform measurement through removal of interconnect dispersion and measurement instrument jitter," IEEE Transactions on Microwave Theory and Techniques, Vol. 50, No. 12, pp. 3022-3028, USA, December 2002.

(continued on the next page)

D. Barataud, F. Blache, A. Mallet, P. P. Bouysse, J.-M. Nébus, J. P. Villotte, J. Obregon, J. Verspecht, P. Auxemery, "Measurement and Control of Current/Voltage Waveforms of Microwave Transistors Using a Harmonic Load-Pull System for the Optimum Design of High Efficiency Power Amplifiers," IEEE Transactions on Instrumentation and Measurement, Vol. 48, No. 4, pp. 835-842, August 1999.

D. Schreurs, J. Verspecht, B. Nauwelaers, A. Barel, M. Van Rossum, "Waveform Measurements on a HEMT Resistive Mixer," 47th ARFTG Conference Digest, pp. 129-135, June 1996.

State-Space Models

Dominique Schreurs, Jan Verspecht, Servaas Vandenberghe, Ewout Vandamme, "Straightforward and Accurate Nonlinear Device Model Parameter-Estimation Method Based on Vectorial Large-Signal Measurements," IEEE Transactions on Microwave Theory and Techniques, Vol. 50, No. 10, pp. 2315-2319, 2002.

John Wood, David Root, "The behavioral modeling of microwave/RF Ics using non-linear time series analysis", International Microwave Symposium Digest 2003 IEEE MTT-S, Vol. 2, pp. 791-794, USA, June 2003.

Scattering Functions

Jan Verspecht, "Everything you've always wanted to know about Hot-S22 (but we're afraid to ask)," Introducing New Concepts in Nonlinear Network Design - Workshop at the International Microwave Symposium 2002, USA, June 2002.

Jan Verspecht, Patrick Van Esch, "Accurately Characterizing Hard Nonlinear Behavior of Microwave Components with the Nonlinear Network Measurement System: Introducing 'Nonlinear Scattering Functions'," Proceedings of the 5th International Workshop on Integrated Nonlinear Microwave and Millimeterwave Circuits, pp. 17-26, Germany, October 1998.